Investigation of seepage around the bucket skirt during installation in sand

Koteras, Aleksandra Katarzyna; Ibsen, Lars Bo

Publication date:
2015

Document Version
Publisher's PDF, also known as Version of record

DEPARTMENT OF CIVIL ENGINEERING
AALBORG UNIVERSITY

Investigation of seepage around the bucket skirt during installation in sand

AAU CPT-based method for the installation of suction bucket

Aleksandra Katarzyna Koteras

Lars Bo Ibsen

ISSN 1901-7278
DCE Technical Memorandum No. 52

Aalborg University

Department of Civil Engineering

Geotechnical Engineering Group

DCE Technical Memorandum No. 52

Investigation of seepage around the bucket skirt during installation in sand

AAU CPT-based method for the installation of suction bucket

by

Aleksandra Katarzyna Koteras
Lars Bo Ibsen

November, 2015

Scientific Publications at the Department of Civil Engineering

Technical Reports are published for timely dissemination of research results and scientific work carried out at the Department of Civil Engineering (DCE) at Aalborg University. This medium allows publication of more detailed explanations and results than typically allowed in scientific journals.

Technical Memoranda are produced to enable the preliminary dissemination of scientific work by the personnel of the DCE where such release is deemed to be appropriate. Documents of this kind may be incomplete or temporary versions of papers—or part of continuing work. This should be kept in mind when references are given to publications of this kind.

Contract Reports are produced to report scientific work carried out under contract. Publications of this kind contain confidential matter and are reserved for the sponsors and the DCE. Therefore, Contract Reports are generally not available for public circulation.

Lecture Notes contain material produced by the lecturers at the DCE for educational purposes. This may be scientific notes, lecture books, example problems or manuals for laboratory work, or computer programs developed at the DCE.

Theses are monograms or collections of papers published to report the scientific work carried out at the DCE to obtain a degree as either PhD or Doctor of Technology. The thesis is publicly available after the defence of the degree.

Latest News is published to enable rapid communication of information about scientific work carried out at the DCE. This includes the status of research projects, developments in the laboratories, information about collaborative work and recent research results.

Table of content:

I. Main report

1. Introduction

Suction caissons have been extensively used in offshore sector as anchors and foundations. Most of experience comes from oil and gas structures. Today, however, the research work proves that this concept is also feasible for offshore wind turbines. The study pays attention on cost- and time-effectiveness, while comparing suction caissons with others foundations recently used for offshore wind turbines*. (Houlsby et al., 2005)* A suction caisson, called here a bucket foundation, is installed through suction applied under the bucket lid. By this means, it can be installed faster and easier, as this method eliminates the use of heavy and expensive driving devices. Nevertheless, the design for the installation process is not straightforward. Firstly, the suction applied to create a driving force has its limitation that need to be preserved. Secondly, while dealing with permeable soil, there is a flow of groundwater around the whole bucket skirt, resulting from the suction. This seepage flow changes the pore pressure, hence the soil stress state. Therefore, the seepage flow requires an analysis, as it influences the soil resistance against the penetration.

The main part of the rapport contains a numerical analysis of seepage development around the bucket foundation during its installation in permeable layer. Different soil combinations are considered with impermeable layer introduced in the soil profiles. Simulations are performed in PLAXIS software. The software is based on the finite element method and it is used for geotechnical problems investigation. Due to simple geometry of bucket foundation, an axisymmetric 2D model is generated. This shortens the time and simplifies the calculus. The process of installation is simulated by static calculation of steady-state seepage for individual steps, where the embedment depth, h, is increasing by 0.1 of bucket diameter, D, for each step. In each such a step it is considered, that the driving force resulting from suction is equal to the soil penetration resistance. By this, it is assumed that there is no penetration as long as there is no increase in driving force. The assumption of discrete stages for installation procedure is therefore justified. The same assumption was used for PLAXIS simulation by *Tran (2006)* and the results were in a good correlation with the experimental results.

First aim of this study is to evaluate a pore pressure factor, α. The factor describes the ratio between the excess pore pressure generated on the bucket tip and the applied suction under the bucket lid. The pore pressure factor can be then used for prediction of excess pore pressure at the tip or along bucket skirt with known soil condition, bucket geometry and applied suction.

The second aim of the study is to evaluate expressions for normalized seepage length, s/h, for different soil combinations and penetration depths. The seepage length is then

used to make a prediction of critical pressure that will create piping channels at exit, which is near to seabed and to the caisson wall, along bucket wall and at the tip. That is how the limits for suction installation can be assumed. Finally, the critical suction is used for predicting the reduction of penetration resistance and the method describing this approach is presented in the report with its assumptions. The method is called AAU CPT-based method and it is a great step in the development of practical design tool for bucket foundation installation process.

2. PLAXIS model for the seepage flow around bucket foundation

2.1. Geometry of bucket foundation

The diameter of bucket is constant, $D = 4$ m. The length of bucket skirts is up to 2 times diameter, which gives 8 m. The penetration length investigated is in the range of 0.1 D to 2.0 D, with interval of 0.1 D. For following analysis the embedment depth, h, is normalized, so it can be used for different geometries. The penetration ratio used further on is a ratio between the penetration depth and the diameter, $0.1 \leq \frac{h}{D} \leq 2.0$.

The bucket foundation in axisymmetric model is simulated by a surface with impermeable interfaces. This assures that the ground water will flow around the bucket skirt and not through it. Surface parameters are not of consideration, as no loading conditions are introduces. Therefore, no material is assigned to the surface. What is more a zero-thickness of bucket skirt, $t_S = 0$, is assumed, as the changes of pore pressure along the skirt tip are not of interest for this study.

Dimensions are shown in Figure 2.1. and the domain with axisymmetric model and used mesh is presented in Figure 2.2. The image of surface interfaces on the inside and outside (called a negative and a positive interface) are indicated in PLAXIS program in the way that can confuse the reader, because there is some thickness between interfaces in the figure. However, this is only the graphical way of presenting the mesh around interface, and there is zero thickness assigned to the bucket skirt for numerical analysis.

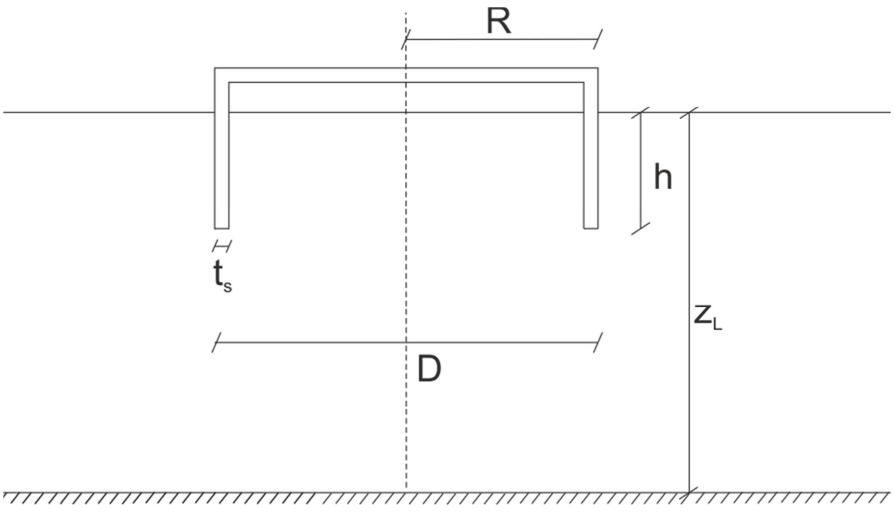

Figure 2.1. *Dimensions definitions*

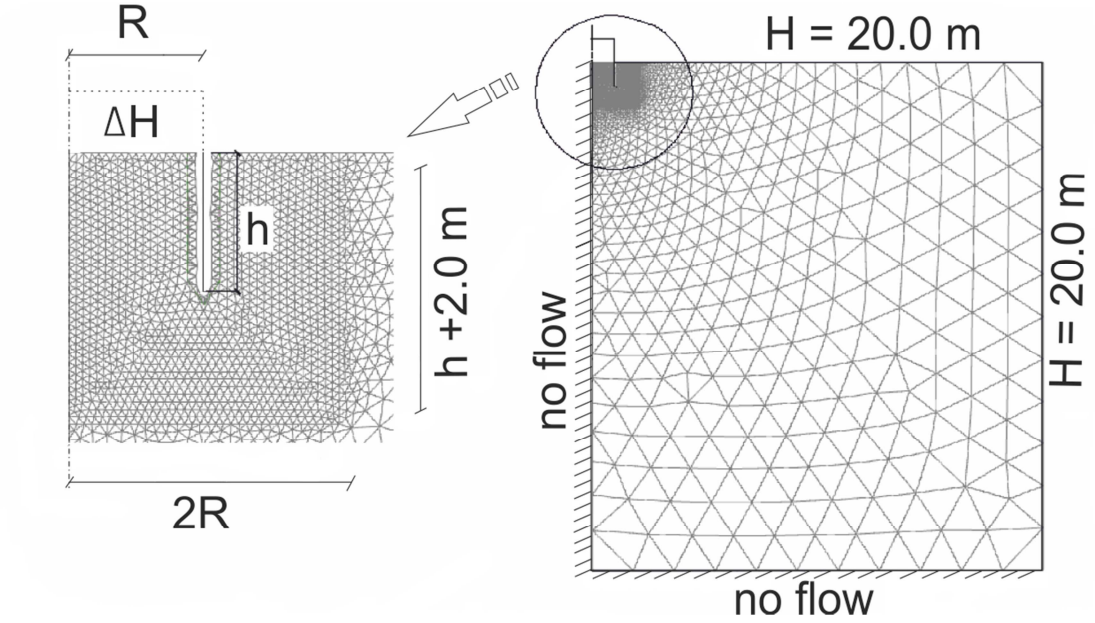

Figure 2.2. *Plaxis domain with final mesh*

2.2. Calculation model and soil parameters

The seepage flow in permeable soil is analyzed with a steady-state groundwater flow calculations. It is performed for each penetration depth defined in section 2.1. The groundwater head for the domain is set as 20 m above seabed and the calculation proceeds until a full-developed seepage state is achieved. The soil is therefore saturated and the only relevant parameter is the coefficient of permeability, k. The USDA series system is chosen for the data set in flow parameters and Van Genuchten model is assigned, however, the model choice is meaningful only for the groundwater flow in unsaturated zones. For fully saturated flow this model describes the flow with Darcy's law.

The permeability chosen for this research is set to default value for Sand type of soil:

$k_{x,y} = 7.128$ m/day.

To simulate the applied suction, a surface groundwater flow boundary is set at the free surface inside the bucket. The hydraulic head at the surface is set lower than the ground water level of the model. In order to achieve the desired suction, there has to be an appropriate head difference, which increases with increasing penetration ratio. The head difference induces the gradient on the bucket skirt wall and the ground water flow is forced; an upward flow in soil plug and downward flow outside the bucket.

The comparison between simulations can be only justifiable, when the same conditions are applied in all of them. This includes the boundary conditions, mesh and calculation phases.

2.3. Boundary conditions

There are three cases that are covered by this study. In the first case the soil profile includes only a homogeneous, permeable soil. In this case the boundaries for the model were chosen to assure no influence on the excess pore pressure around the bucket skirt from the boundaries. The outer boundary was set to be 40 m, which is 10 times the diameter length. It is ensured that this boundary does not affect pore pressure results in any of simulations. The bottom boundary was set to be 45m, based on domain size convergence analysis. The same conditions were sufficient for the second case, where the permeable layer is situated under the impermeable layer. Results are presented in section *2.5. Domain size convergence analysis.* For the third case, where the permeable layer is situated above the impermeable layer, the bottom boundary is determined by the distance to impermeable layer, z_L , see *Figure 2.1.*

The groundwater flow boundary conditions for entire model are assigned. First, at the axi-symmetric boundary and at the bottom boundary the flow through them is prevented. The free surface and outer boundary have prescribed pore pressure, resulting from established ground water level. However, the head at free surface inside the bucket, simulating the cavity under the bucket lid, is set according to desire suction giving an appropriate head difference. At the free surface outside, the head of 20m is set, the same as for entire domain. The boundary conditions can be seen in Figure 2.2.

For the case where impermeable layer is placed at the top, the flow is prevented at the free surface outside the bucket. The flow through surface used as bucket skirt is prevented.

2.4. Mesh and calculation phases

The model is meshed with the refining factor that assures the preciseness. Elements distribution is achieved with a medium mesh of entire model. However, as the main interest of this study is the area around the bucket skirt, therefore it is more refined with coarseness factor of 0.03125. The same coarseness factor is assigned to the surface that simulates the bucket skirt. As a result, the pore pressure can be extracted with more accuracy along the bucket wall.

The refined area is of 4 m width, 2 m distance from the bucket skirt, and of length h + 2 m, 2 m from the bucket tip, see *Figure 2.2.*

The calculation phases are as following:

- Initial phase

Only soil volume is activated and the pore pressure in the soil is calculated based on phreatic level. A 'Groundwater flow only' type of calculation is chosen.

- Calculation phase: suction

Next to activated soil from initial phase, the surface that simulates the bucket skirt with its interfaces is activated. A 'Steady state groundwater flow' calculation type is chosen, so it is time-independent. The behavior of flow boundary conditions are specified in the Object explorer in PLAXIS program, see figure 2.3., *(Brinkgreve, 2012):*

- the interfaces on the surface are set to be impermeable,
- the behavior of the flow boundary condition at free surface inside the bucket is set as 'Head' and an appropriate value of head is defined,
- rest of flow boundaries are set according to section *2.3 Boundary condition.*

The changes in pore pressures due to applied head difference are calculated based on hydraulic conditions. Pore pressures from nodes on the interfaces are used for seepage flow analysis around the bucket skirt.

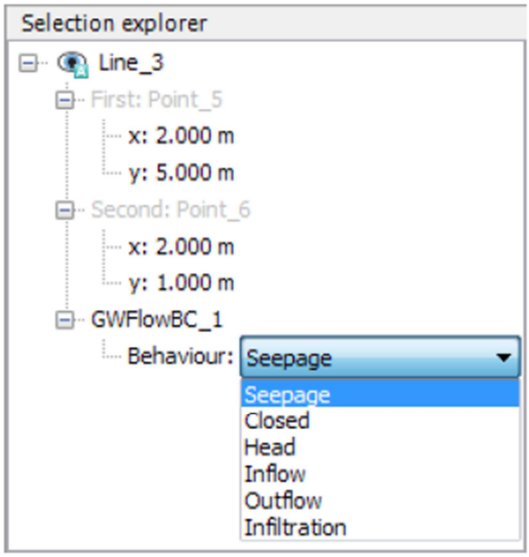

Figure 2.3. The available options of behavior of groundwater flow boundary conditions

2.5. Domain size convergence analysis

A domain size convergence analysis is performed for cases with h/D = 0.1 and $\frac{h}{D}$ = 2.0. Changes in pore pressure factor are investigated in relation to the distance to bottom of permeable layer. The research proves that the impermeable layer below sand is influencing the flow in sand, and that influence is dependent on the distance to this layer. For case of homogenies sand, case (a), and case of impermeable layer above sand, case (b), it should be ensured that the bottom boundary has no influence on excess pore pressure around the bucket skirt. Results of convergence analysis for both cases, see Figure 2.4., are showed in *Figure 2.5.* for h/D = 0.1 and *Figure 2.6.* for $\frac{h}{D}$ = 2.0.

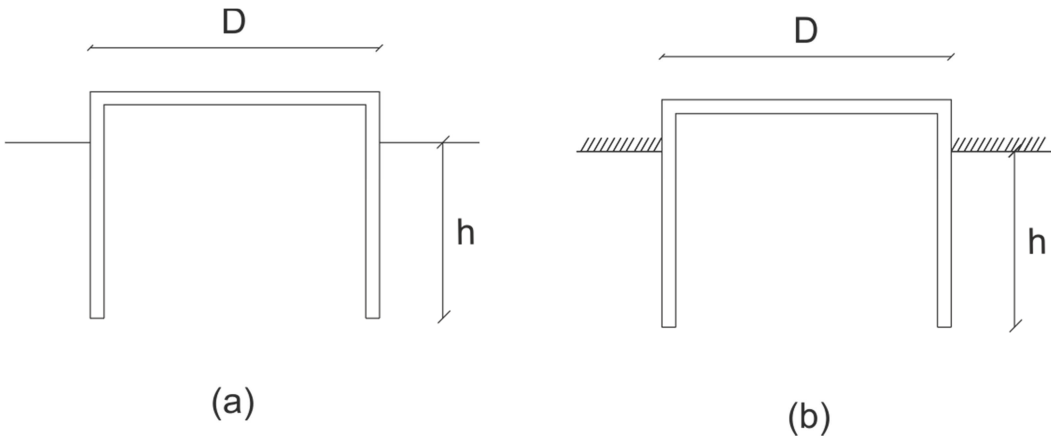

Figure 2.4. *Cases used for domain convergence analysis*

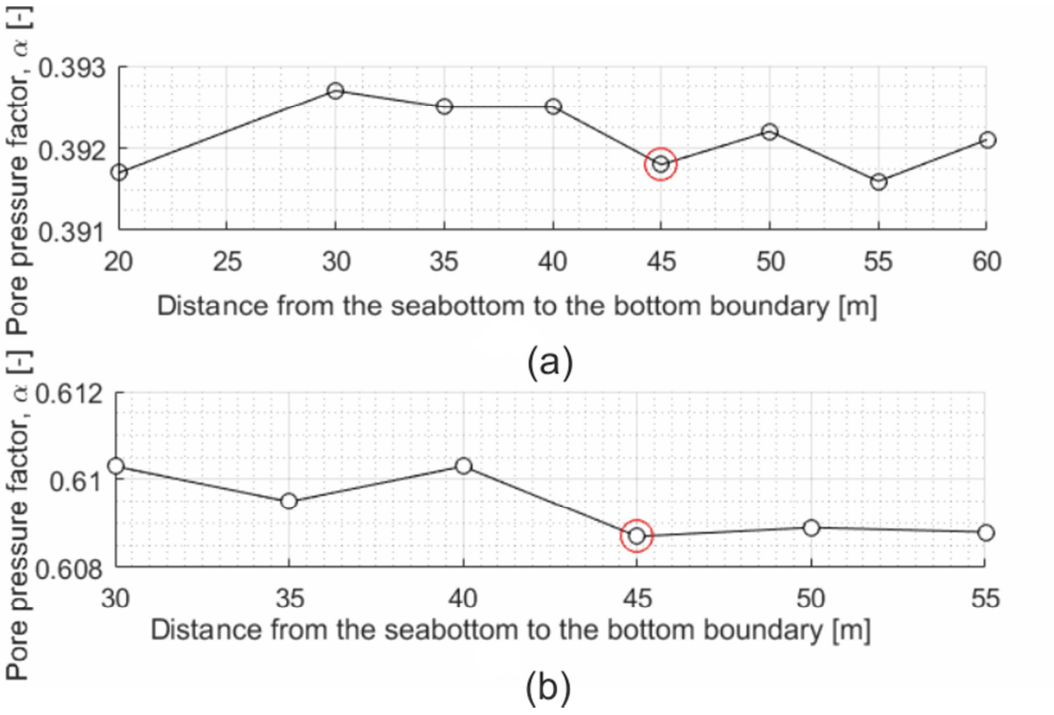

Figure 2.5. *Convergence analysis results for* $h/D = 0.1$

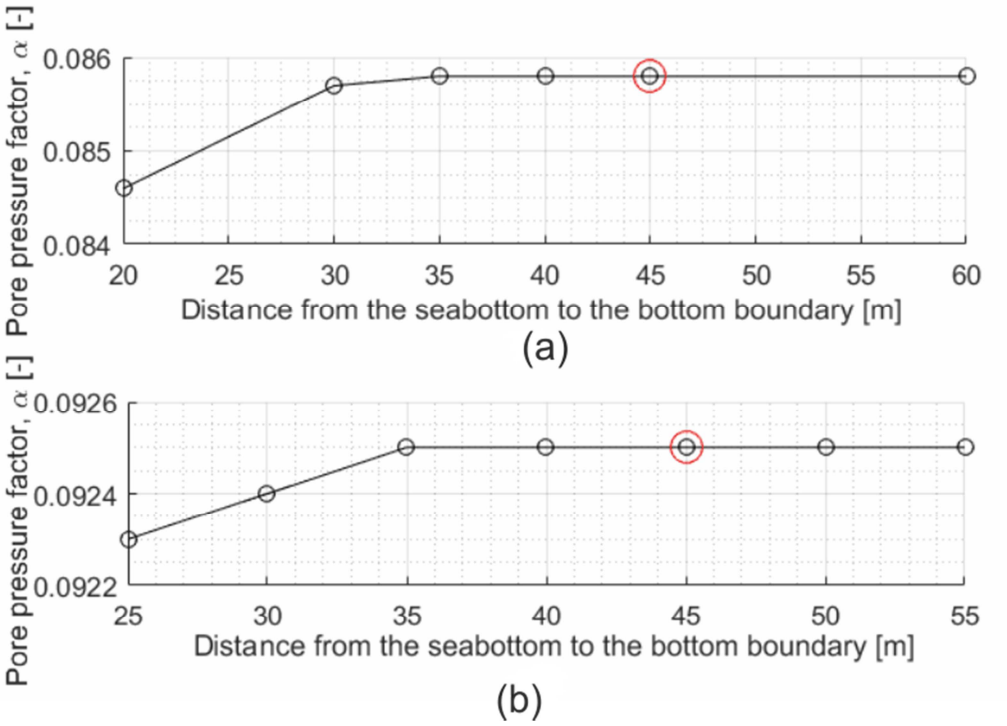

Figure 2.6. *Convergence analysis results for h/D = 2.0*

As a result of analysis, the bottom boundary is set to be 45 m. The point of convergence is highlighted on figures with red circles.

The convergence analysis on the number of elements is not presented here, because the refined meshed around the bucket skirt is set with the highest refining factor, so that results on the interfaces can be read as close to the tip of skirt as possible. It might be that the refining required for results to converge is less that it is chosen, but the results of pore pressure on interfaces are of the most importance and therefore the highest refining is chosen.

2.6. Assumptions and limitations

As mentioned before, even though the installation of bucket foundation is a continuous process, it is simplified by stages, in which the penetration depths are increasing and steady state flow is assumed. However, this indicates that the approach cannot be used for assessing the suction installation, when the rate of pumping is high, as this might result in seepage flow not to be fully developed.

What is more, the seepage flow might change the permeability of the soil around the bucket. It is, however, assumed that the permeability is uniform during the installation process.

3. Theory for analyzing the numerical results

3.1. Extracting results from PLAXIS 2D simulations

Results of exit flow velocity and of excess pore pressure around the bucket skirt are extracted from PLAXIS 2D after each simulation. The excess pore pressure are extracted at the exit inside the bucket (applied suction), the exit outside the bucket and at the tip in order to calculate the average hydraulic gradient at inside and outside skirt. Then the excess pore pressure as near to the tip as possible, on the inside and outside skirt in order to calculate hydraulic gradient around the tip. The flow velocity extracted at the exit inside the bucket is used for calculation of exit hydraulic gradient. Extraction points for those results are highlighted in Figure 3.1.

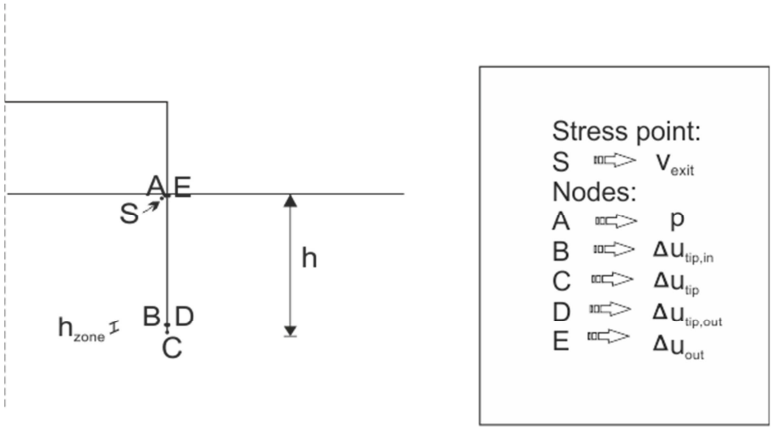

Figure 3.1. Nodes for extracting the excess pore pressures on positive and negative interfaces and stress point for extracting exit velocity

The point of extraction the exit velocity is a soil stress point and it is found in a distance of 1 cm from the free surface and of 1 cm from the skirt. Excess pore pressures are extracted from nodes on the interfaces. It is secured that the point of extraction of pore pressure close to the bucket tip is for all simulations at the distance between 2 – 3 cm from the tip.

3.2. Pore pressure factor, α

A pore pressure factor is calculated as a ratio of the excess pore pressure measured at the tip of bucket skirt to the applied suction and is found for all penetration ratios.

$$\alpha = \frac{\Delta u_{tip}}{p} \tag{3.1}$$

Where

p	Applied suction	[kPa]
Δu_{tip}	Excess pore pressure at the tip of bucket skirt	[kPa]

The suction is of a magnitude dependent on a groundwater head difference between a general groundwater level established for a model and a head prescribed to the groundwater flow boundary condition at the free surface inside the bucket. The suction is then calculated with following equation.

$$p = \left(H - H_{ref}\right) \cdot \gamma_w \tag{3.2}$$

where

H	General groundwater level	[m]
H_{ref}	Prescribed head for groundwater flow boundary condition at free surface	[m]
γ_w	Unit weight of water	[kN/m^3]

The excess pore pressure is calculated as a difference between the hydrostatic pore pressure based on general groundwater head and the pore-water pressure that appears after the suction is applied, see following equation.

$$p_{excess} = p_{hydrostatic} - \ p_{water} \tag{3.3}$$

where

$p_{hydrostatic}$	Hydrostatic pressure	[kPa]
p_{water}	Pore-water pressure	[kPa]

The applied suction in all simulations for homogeneous soil is chosen in the way to ensure a value close to the critical one, but never exceeding it. However, the analysis revealed, that even when smaller values of suction are applied, the pore pressure factor is not affected by that, indicating that the pore pressure factor holds for any value of suction to be applied.

3.2.1. Literature review

A method for determining the soil penetration resistance for caisson foundation installation in sand with and without suction assistance was proposed by *(Houlsby and Byrne, 2005).* The method is based on pore pressure gradients resulting from applied suction. It is stated, that the pore pressure factor for the tip is expected to be less than 0.5 as the flow is more restricted inside than outside the caisson. The article points out that the suction applied causes a loosening of sand inside the caisson, hence changing the permeability inside. Based on results from two different numerical studies the following expression for pore pressure factor is given, assuming uniform permeability,

$$\alpha_0 = \ 0.45 - 0.36 \cdot \ (1 - \exp(-\frac{h}{D \cdot 0.48})\ ) \tag{3.4}$$

The pore pressure factor in layered soil was investigated by Christian LeBlanc as a part of his PhD research at Aalborg University. Oliver Cotter, *(Cotter, 2009)*, relates in his work to personal conference with LeBlanc, where, based on numerical analysis on suction bucket installation performed in FLAC 3D, the solution for pore pressure factor for case with impermeable layer under the permeable soil is given.

$$\alpha = \alpha_0 + 0.15 \cdot \frac{h}{D} \cdot \left(\left(\frac{h}{z_L} \right)^2 + \frac{D}{z_L} - 1 \right) \tag{3.5.}$$

Both solutions presented in this section are derived for penetration ratio up till 1.2 only. Given expression are plotted in figure below.

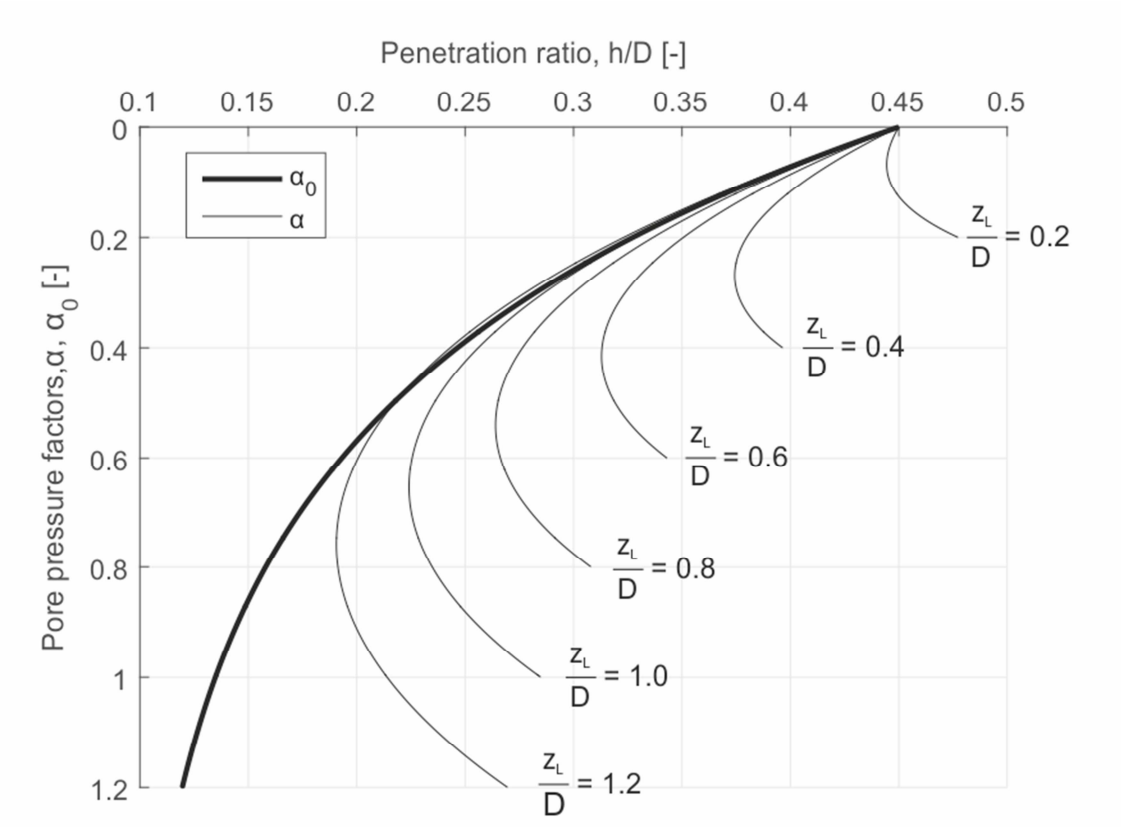

Figure 3.2. Solution for pore pressure factor for homogenies soil and for case with impermeable layer below proposed by *Houlsby and Byrne (2005)* and LeBlanc (2009)

3.3. AAU CPT-based method for installation of bucket foundation

The AAU CPT-based method is an approach, where the soil penetration resistance is assumed to be related to the cone resistance, q_c, measured during Cone Penetration Test, CPT. The recommendation for such a practice is found in *(DNV, 1992)*. The method presented in this section has been developed by the Department of Civil Engineering at Aalborg University, Denmark.

The penetration resistance of the soil is calculated in depth intervals, so that different soils in varying soil profile can be included. The cone resistance is related to the soil resistance, tip resistance and friction at the skirt, through empirical coefficients k_p and k_f respectively. Furthermore, this method takes into account the changes in soil resistance due to the seepage flow, what is not included in DNV practice. The changes in soil resistance resulting from seepage are introduced by β-factors. Those factors, together with the average cone resistance and empirical coefficients are derived for each depth interval, see Figure 3.3.

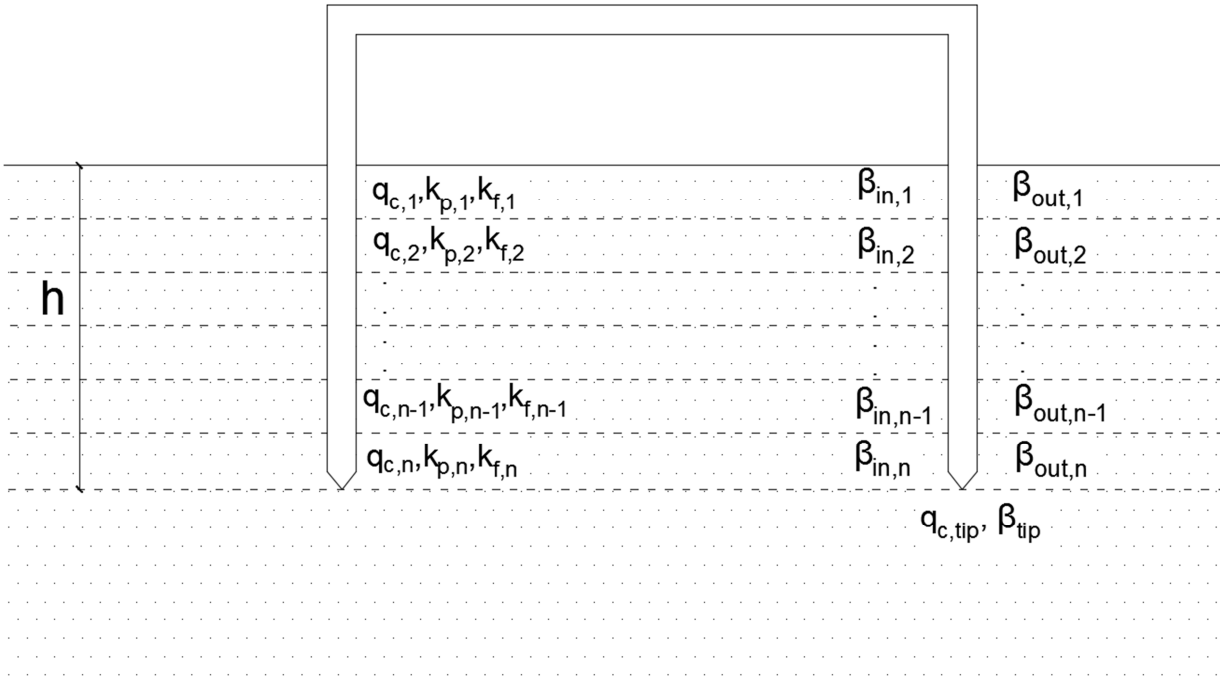

Figure 3.3. Parameters for calculation of soil penetration resistance

It is recommended to perform two calculations which include the most probable and the highest expected soil resistance throughout appropriate coefficients. For North Sea conditions coefficients for dense sand and stiff clay are proposed, see Table 3.1. Additionally it is noted that the values of k_p and k_f for the upper 1 - 1.5 m should be 25 - 50 % lower than those from *Table 3.1.* This is due to local piping and lateral movement of structure. Moreover, the increase in tip area influences the value of k_f,

what results in reduced value. For soil conditions that indicate sand/clay mixture, values of k_p and k_f should be somehow between those values given in the *Table 3.1.*

Table 3.1. Values for empirical coefficient for soil penetration resistance, North Sea conditions. (DNV,1992)

Type of soil	*Most probable*		*Highest expected*	
	k_p	k_f	k_p	k_f
Clay	0.4	0.03	0.6	0.05
Sand	0.3	0.001	0.6	0.003

The total soil penetration resistance is calculated as a sum of tip resistance and friction between soil and skirt.

$$R_{tot} = F_{in} + F_{out} + Q_{tip} \tag{3.6}$$

where

R_{tot}	The total soil penetration resistance	[kN]
F_{in}	Friction between soil and inner side	[kN]
F_{out}	Friction between soil and outer side	[kN]
Q_{tip}	Tip resistance	[kN]

The friction between soil and skirt is calculated using the average value of cone resistance for a small depth interval, $q_{c,i}$. However, for homogenies soil the integrated value of cone resistance over the penetration depth should be used.

$$F_{in,i} = k_{f,i} \cdot \beta_{in,i} \cdot q_{c,i} \cdot A_{s,in,i} \tag{3.7}$$

$$F_{out,i} = k_{f,i} \cdot \beta_{out,i} \cdot q_{c,i} \cdot A_{s,out,i} \tag{3.8}$$

$$Q_{tip}(h) = A_{tip} \cdot k_p \cdot \beta_{tip}(h) \cdot q_c(h) \tag{3.9}$$

where

β	Factor related to the change in resistance due to seepage	[-]
$A_{s,in,i}$	Skirt inside area for given interval	[m^2]
$A_{s,out,i}$	Skirt outside area for given interval	[m^2]
$A_{tip,i}$	Tip area of skirt	[m^2]
h	Penetration depth	[m]

The first stage of penetration is due to self-weight of bucket foundation. It is required that the bucket is installed till required depth before the suction can be applied. This

depth is dictated by the condition that a sufficient seal between the skirt and the soil is ensured. Further installation requires application of suction.

The penetration of the bucket for given penetration depth is controlled by following equation.

$$W_{total}(h) + p(h) \cdot A_{lid} \geq F_{in}(h) + F_{out}(h) + Q_{tip}(h) \tag{3.10}$$

where

W_{total}	Weight of the bucket reduced for buoyancy	[kN]
p	Suction pressure applied under the bucket lid	[kPa]
A_{lid}	Area of the bucket lid on which suction is applied	[m^2]

By rewriting *equation (3.10),* the solution for required suction is obtained.

$$p_{req}(h) = \frac{W_{total}(h) + R_{tot}(h)}{A_{lid}} \tag{3.11}$$

The suction applied under the bucket skirt in permeable soil results in seepage flow around the bucket skirt, whereas in less permeable soil this effect is limited. The hydraulic gradient that appears in soil changes the soil stress state. The downward gradient increases the soil effective stress, whereas the upwards gradient decreases them. The increased/decreased value of effective soil stress due to seepage can be assumed as:

$$\sigma_{seepage} = \gamma' \cdot z \pm i \cdot \gamma_w \cdot z \tag{3.12}$$

where

γ'	Submerged unit weight of soil	[kN/m^3]
γ_w	Unit weight of water	[kN/m^3]
i	Hydraulic gradient	[-]
z	Depth	[m]

Figure 3.4. presents the change in groundwater head as a result of applied suction under the bucket lid in soils with different coefficient of permeability based on soil model in PLAXIS 2D. The penetration ratio is equal to 1.0. Case (a) represents sandy soil with high permeability, in case (b) slightly decreased permeability is used and in case (c) permeability value characteristic for clayey silt is used. In each case the same suction is applied under the bucket lid, $p = (20 - 14.8) \cdot \gamma_w$ kPa, which comes from the hydraulic head difference inside and outside the bucket. In each case, the same time interval is used for seepage to develop.

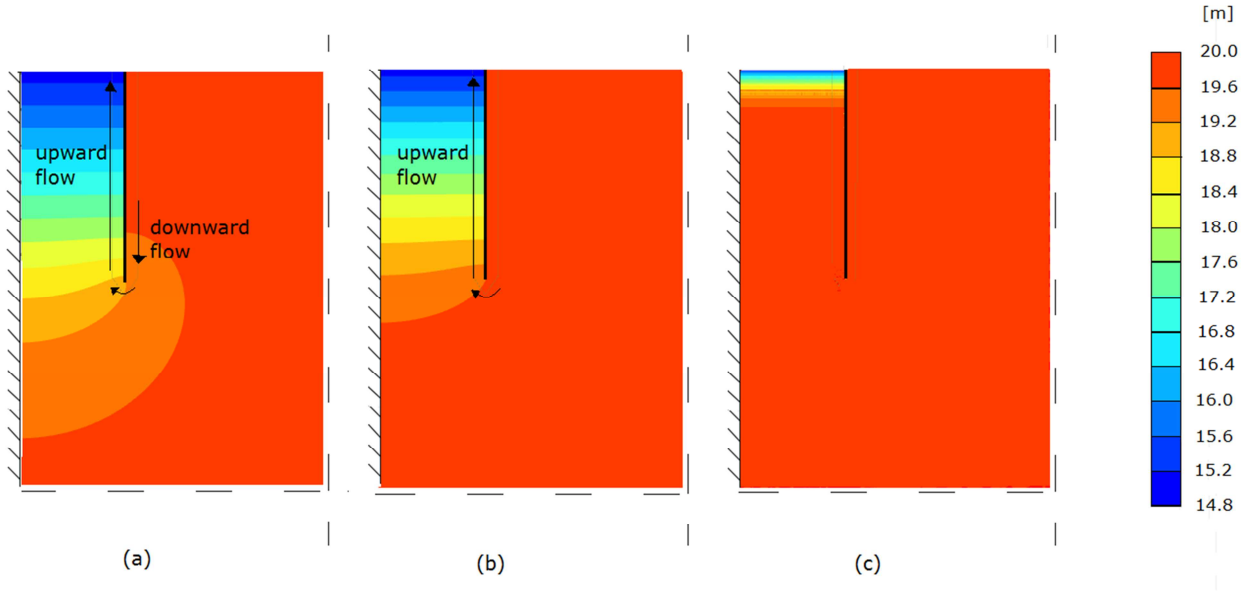

Figure 3.4. The groundwater head for applied suction: (a) sand, (b) silty-sand and (c) clay, with approximated flow line

When there is a difference in hydraulic head within the soil, a seepage flow occurs. The flow lines are perpendicular to the equipotential line and the ground water flows from a point of bigger potential to a point with smaller potential (from bigger to smaller hydraulic head). The upward flow of pore water that takes place inside the bucket reduces the effective soil stress. Such a loosening of soil decreases the penetration soil resistance and as a result, less force is required to penetrate the bucket. The most of reduction is expected in case (a) where a high hydraulic gradient at the inside wall and at the tip occurs. In case (b) the hydraulic gradient is smaller at the inside wall and almost disappear at the tip. Therefore, less reduction in soil resistance is expected. Finally, almost no flow occurs in case (c), and therefore, the reduction of penetration resistance should not be included in installation design for impermeable soil. The study described in this report included only seepage flow in soil with high permeability, where the seepage development is expected for small time intervals.

The phenomena of seepage inside the bucket is beneficial for the installation procedure, however, complete loss in soil resistance forms piping channels. As a result, the seal between the soil and bucket skirt is broken and no further penetration can be performed. Therefore, it is extremely important to investigate the critical suction pressure for the bucket foundation installation. The penetration resistance is reduced to zero, when the hydraulic gradient reaches its critical value,

$$i_{crit} = \frac{\gamma'}{\gamma_w} \tag{3.13}$$

and in such a case, β-factor is equal to zero. On the other hand, where no suction is applied, there is no flow of groundwater and no reduction ($\beta = 1$).

3.3.1. β – factors for reduction of soil penetration resistance

β-factor for presented method is proposed to be a function of the ratio between the applied suction during the installation and the critical pressure based on an appropriate hydraulic gradient for each penetration depth. The function includes also a factor r that is expected to be dependent on permeability and the rate of penetration and is set to be in a range of 0 - 1. For homogeneous sand, where permeability is high and the penetration rate is 1 m/hour this factor is equal to 1.0 and for impermeable soil, where no flow occurs, it is equal to 0. β-factor for less permeable soil, where the development of seepage requires longer time interval, is increased as r is somewhere between 0 – 1.0. As β-factor is closer to 1.0, there is less reduction of soil penetration resistance. Following equations are used for determining β-factors.

$$\beta_{avq,in} = (1 - r \cdot \frac{p}{p_{crit,avg,in}}) \quad \text{for } p \leq p_{crit} \tag{3.14}$$

$$\beta_{tip} = (1 - r \cdot \frac{p}{p_{crit,tip}}) \quad \text{for } p \leq p_{crit} \tag{3.15}$$

$$\beta_{avq,out} = (1 + r \cdot \frac{p}{p_{crit,avg,out}}) \quad \text{for } p \leq p_{crit} \tag{3.16}$$

The study on r value includes the numerical investigation and calibration with large-scale tests results of bucket installation. However, the study on this is still ongoing and the results are expected to be published as a next step of the research.

3.4. Normalized seepage length and critical suction

The prediction of critical pressure is based on calculated values of seepage length for each considered hydraulic gradient. The seepage length is calculated with a use of following equation *(Senders & Randolph, 2009)*.

$$s = \frac{p}{\gamma_w \cdot i} \tag{3.17}$$

p	Any applied suction under the bucket lid	[kPa]
i	Any hydraulic gradient due to applied suction	[-]

The critical pressure is then calculated by implementing the critical hydraulic gradient into equation (3.17).

$$p_{crit} = s \cdot \gamma_w \cdot i_{crit} = s \cdot \gamma' \tag{3.18}$$

The study includes analysis of seepage lengths based on the exit, the average and the tip hydraulic gradient. The exit hydraulic gradient is based on the velocity of the flow extracted inside the bucket, as closed as possible to the bucket skirt and to the free surface, see Figure 3.1. The exit gradient is calculated with following equation.

$$i_{exit} = \frac{v_{exit}}{k} \tag{3.19}$$

Where

v_{exit}	Velocity of water flow extracted close to the bucket wall at the exit	[m/day]
k	Coefficient of permeability	[m/day]

For the average hydraulic gradient inside and outside the bucket and the hydraulic gradient at the tip the excess pore pressures from interfaces are used. The gradient is then obtained as:

$$i_{avg,in} = \frac{p - \Delta u_{tip}}{h \cdot \gamma_w}, \quad (3.20)$$

$$i_{avg,out} = \frac{\Delta u_{tip} - \Delta u_{out}}{h \cdot \gamma_w}, \quad (3.21)$$

$$i_{tip} = \frac{\Delta u_{tip,in} - \Delta u_{tip,out}}{2 \cdot h_{zone} \cdot \gamma_w}, \quad (3.22)$$

where

Δu_{out}	Excess pore pressure outside the caisson at level of seabed,	[kPa]
$\Delta u_{tip,in}$	Excess pore pressure on the inside of the caisson, close to the tip,	[kPa]
$\Delta u_{tip,out}$	Excess pore pressure on the outside of the caisson, close to the tip,	[kPa]
h_{zone}	Distance from the tip to the point of extraction of pressure for $\Delta u_{tip,in}$ and $\Delta u_{tip,out}$.	[m]

The results from all hydraulic gradients reveal that it is at the tip where the hydraulic gradient first becomes critical. However, it is stated that even though the critical hydraulic gradient occurs first at the tip of the caisson, it is not the one that controls when piping occur, because the sand at the tip is constrained by the surrounding material. It is in fact the exit gradient adjacent to the bucket skirt which controls the piping, and therefore, should be used for estimation of critical suction for installation.

The seepage length is normalized and presented as a ratio between the seepage length and the embedment depth, $\frac{s}{h}$.

3.4.1. Literature review

The exit normalized seepage length based on numerical simulations performed in FLAC3D has been presented as a close form solution, *(Ibsen and Thilsted, 2010).*

$$\left(\frac{s}{h}\right)_{ref} = 2.86 - \arctan\left(4.1 \cdot \left(\frac{h}{D}\right)^{0.8}\right) \cdot \left(\frac{\pi}{2.62}\right) \quad (3.23)$$

The solution is only valid for penetration ratio $0.1 \leq \frac{h}{D} \leq 1.2$. The steady-state flow simulations were performed on an axisymmetric model.

Additional the case of sand over impermeable soil was investigated, with varying distance to the close bottom boundary. The results of the normalized seepage length were fitted to the following equation.

$$\left(\frac{s}{h}\right) = \left(\frac{s}{h}\right)_{ref} + 0.1 \cdot \left(\frac{D}{z_L}\right) \cdot \left(\frac{h}{z_L - h}\right)^{0.5} \tag{3.24}$$

The normalized critical pressure is given as:

$$\frac{p_{crit}}{\gamma' \cdot D} = \frac{h}{D} \cdot \left(\frac{s}{h}\right) \tag{3.25}$$

Results of normalized seepage are presented in figure below.

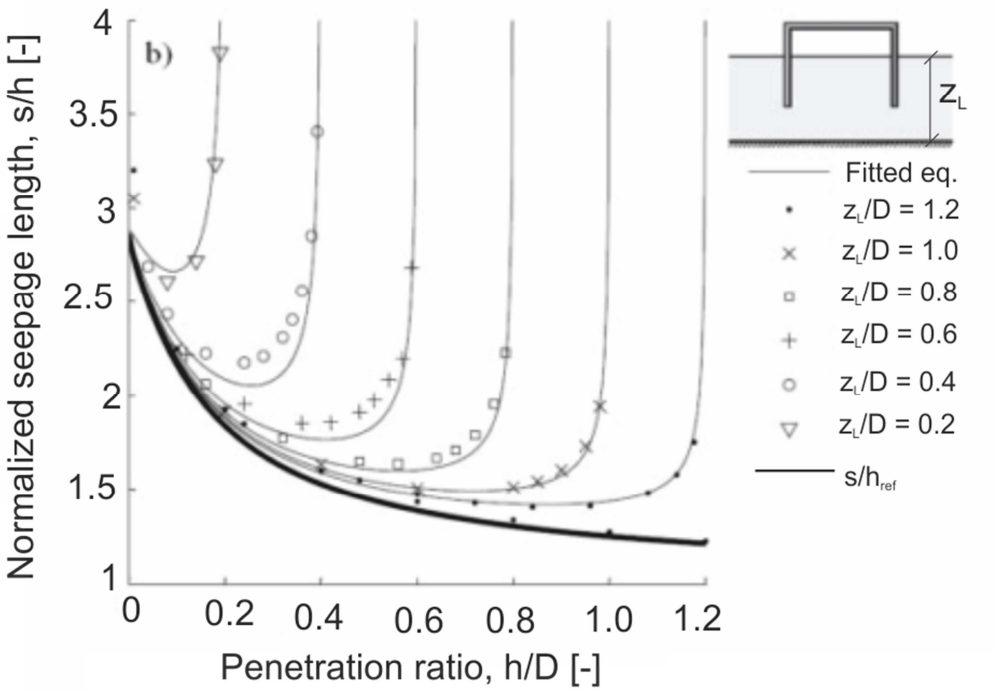

Figure 3.5. *Normalized seepage for homogenies sand and for impermeable layer under sand, (Ibsen and Thilsted, 2010)*

Tove Feld, *(Feld, 2001)*, based on simulations from the finite element program SEEP proposed the estimation for normalized critical suction as following:

$$\frac{p_{crit}}{\gamma' \cdot D} = 1.32 \cdot \frac{h}{D}^{0.75}. \tag{3.26}$$

This equation gives estimation for normalized seepage to be:

$$\frac{s}{h} = 1.32 \cdot \frac{h}{D}^{-0.25}. \tag{3.27}$$

The solution for seepage length based on results from numerical simulations in PLAXIS and SEEP and from the results from theoretical solution for a sheet-pile wall is given also by *equation (3.28)*, *(Senders and Randolph, 2009*).

$$\left(\frac{s}{h}\right)_{ref} = \pi - \arctan\left(5 \cdot \left(\frac{h}{D}\right)^{0.85}\right) \cdot \left(2 - \frac{2}{\pi}\right) \tag{3.28}$$

All three solutions for normalized seepage are presented in figure below.

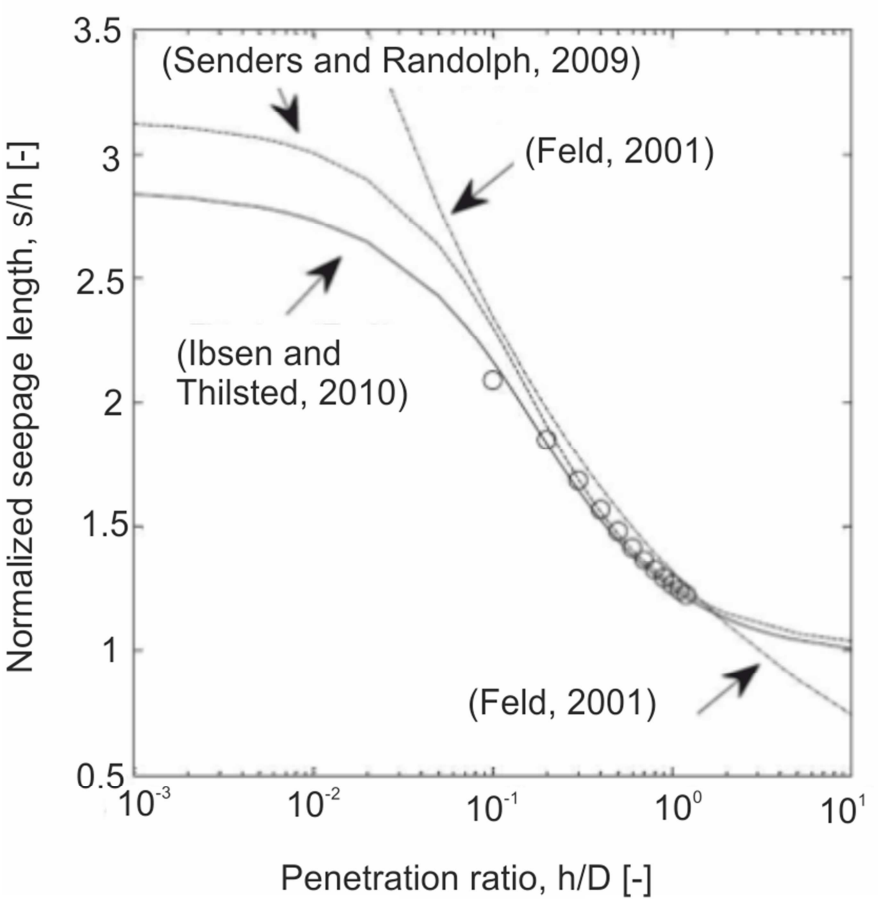

Figure 3.6. Solutions for normalized seepage, comparison (Ibsen and Thilsted, 2010)

3.5. Procedure for calculation of β- factors based on numerical results

The procedure is shown in Figure 3.7. as a flow chart with all steps listed .

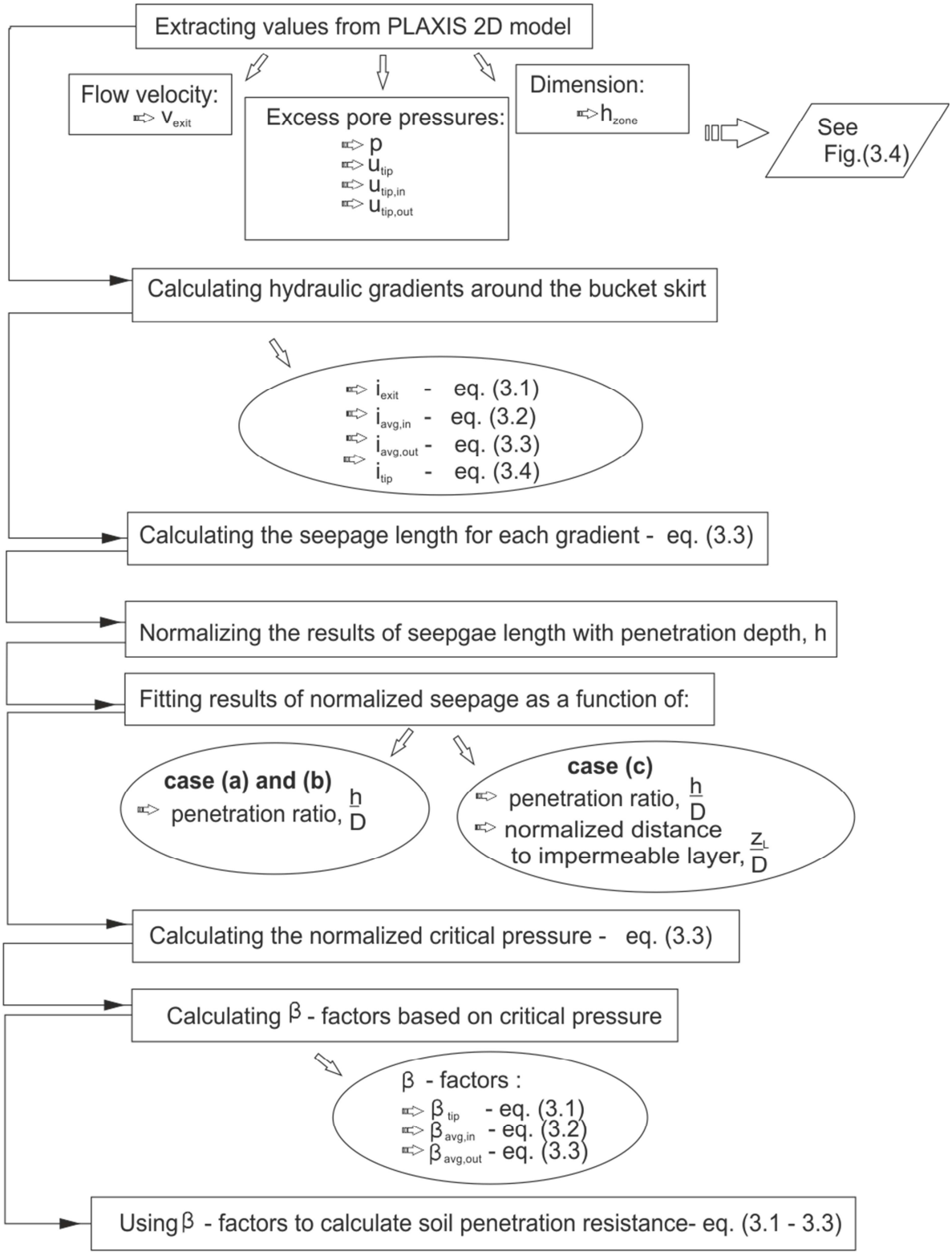

Figure 3.7. AAU CPT-based method for calculation of soil penetration resistance for bucket installation – flow chart

4. Results from numerical analysis

4.1. Case of homogenies permeable soil (a)

The soil profile used includes only a homogenies permeable soil, sand. The boundary conditions and model and soil properties are described in chapter 2. The theory used for deriving the results is described in chapter 3.

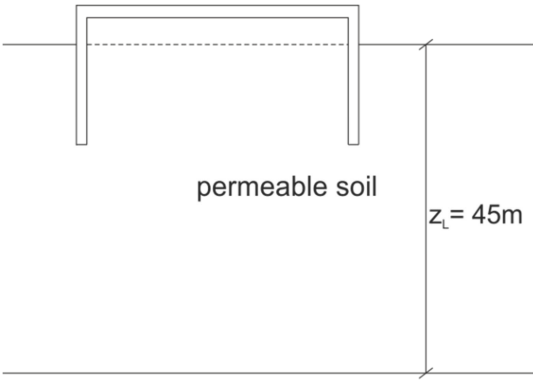

Figure 4.1. Case of homogenous permeable soil

The graphs below show the excess pore pressure changes induced by suction for penetration ratio equal to 0.1, 0.5 and 1.0, *Figure 4.2.* It can be concluded, that the hydraulic gradient at the inside skirt and at the tip is much bigger for increasing penetration ratio. Therefore, the reduction of soil resistance at the beginning of the installation is expected to be small. When the bucket penetrates deeper, less suction is required to achieve significant reduction in penetration resistance.

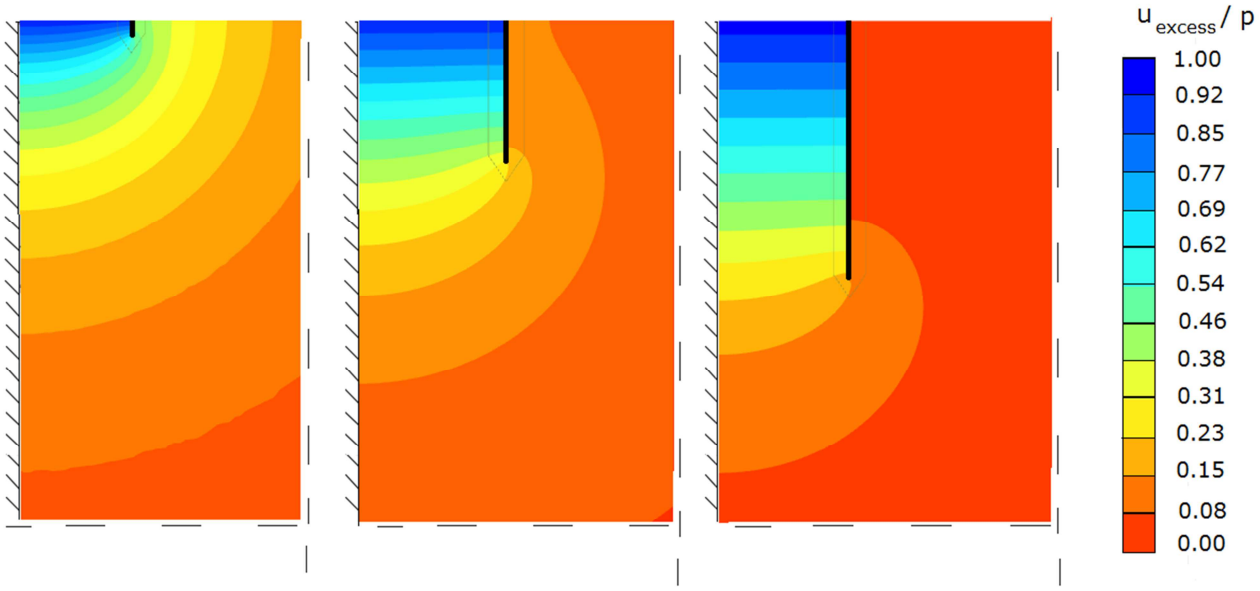

Figure 4.2. Results of ratio between excess pore pressure and applied suction under the bucket lid for $h/D = 0.1, 0.5$ and 1.0.

The results of pore pressure factor obtained from numerical analysis are plotted together with *equation (3.4)*, proposed by *Houlsby and Byrne (2005*), see *Figure 4.3.* The function fits well with numerical results. This fit is better for penetration ratio up to 0.5, but it seems like it can be improved for increasing penetration ratio.

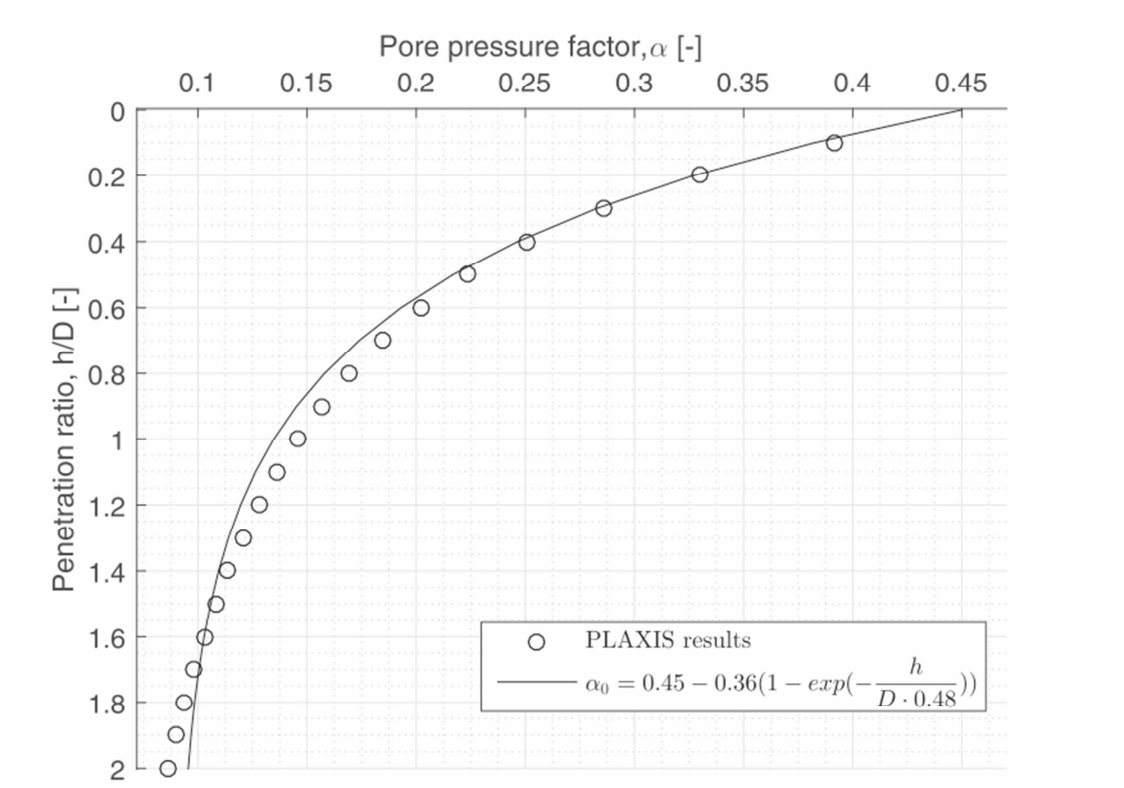

Figure 4.3. *Results of pore pressure factor plotted versus penetration ratio* with expression from *(Houlsby and Byrne, 2005)*

The best fit was found by investigating different functions. The simple, rational expression was found as an excellent fit for numerical results, *equation (4.1)*. The coefficient of determination, R^2, is found to be 0.9999.

$$\alpha_0 = = \frac{a}{\frac{h}{D} + b} \tag{4.1}$$

where

a	0.21
b	0.44

Figure 4.4. presents a case for homogenies sand with chosen solution.

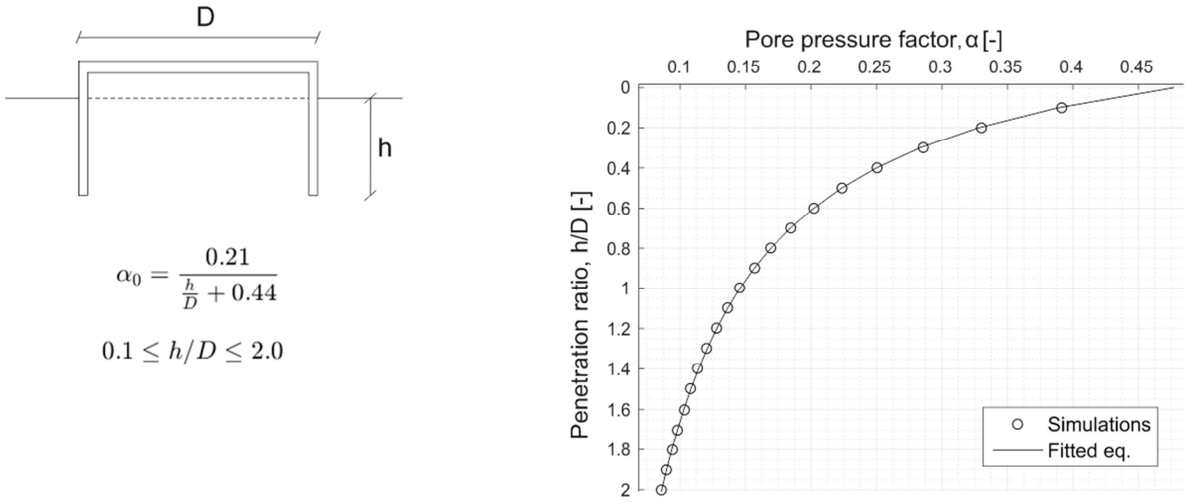

Figure 4.4. *Results of pore pressure factor versus penetration ratio along with chosen solution*

For normalized seepage length the results obtained from numerical simulations are plotted together with solutions proposed by other researchers, see *Figure 4.5.*

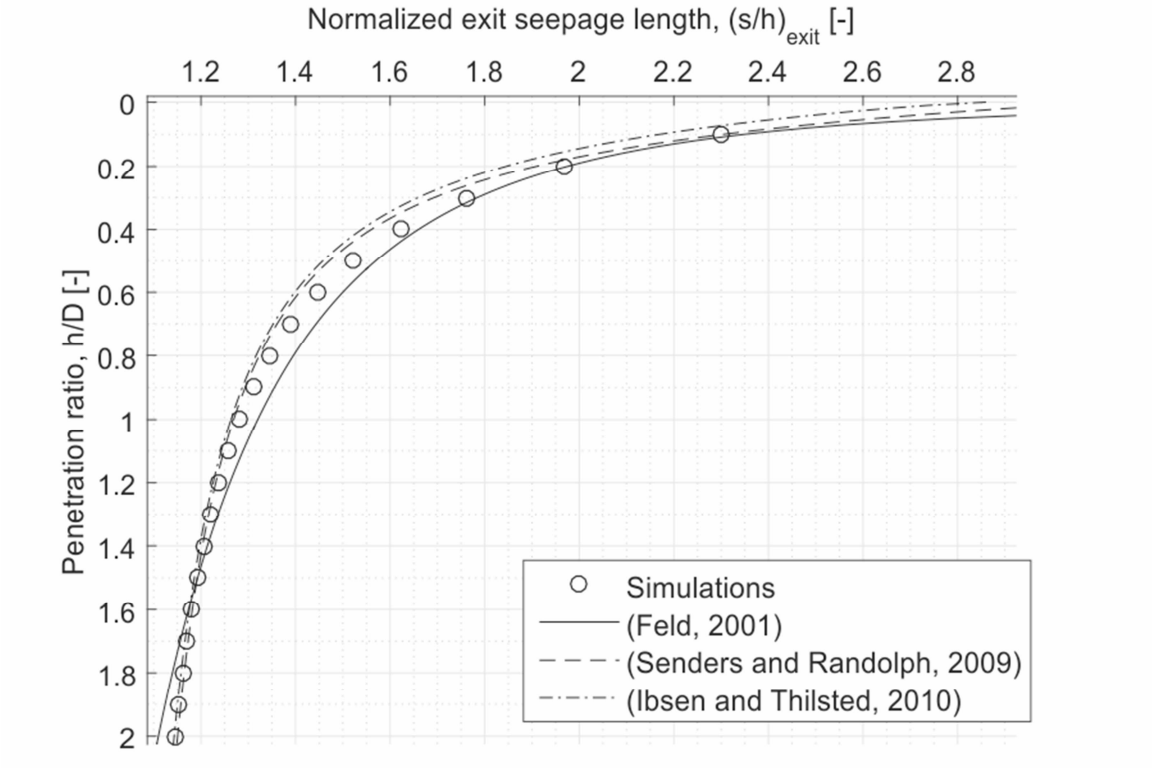

Figure 4.5. *Results of normalized seepage length for exit gradient versus penetration ratio along with solutions from literature*

Better fitting is obtained for arctangent functions. Therefore constants and exponent are adjusted, so that the best fit is obtained with values given below, where $R^2 = 0.9995$.

$$\left(\frac{s}{h}\right)_{exit} = \pi - \arctan\left(a \cdot \left(\frac{h}{D}\right)^b\right) \cdot (2 - \frac{c}{\pi}) \quad (4.2)$$

a	3.6
b	0.74
c	-1.8

The equation for normalized seepage length for exit gradient is taken as a reference equation, $\left(\frac{s}{h}\right)_{ref} = \left(\frac{s}{h}\right)_{exit}$, and it is used for fitting for different gradients and in different soil conditions.

For average hydraulic gradient inside the caisson and the tip gradient, following expression is used for fitting.

$$\left(\frac{s}{h}\right) = a \cdot \left(\left(\frac{s}{h}\right)_{ref} - b\right) + 1 \quad (4.3)$$

Constants found for both gradients and R^2 values are presented in *Table 4.1.*

Table 4.1. Fitted constants for *equation 4.3* and R^2values

	for exit gradient	*for average gradient*	*for tip gradient*
a	1	0.46	0.27
b	1	0.9	3.9
R^2	0.9995	0.9957	0.9739

Results are presented in Figure 4.6. along with chosen solutions.

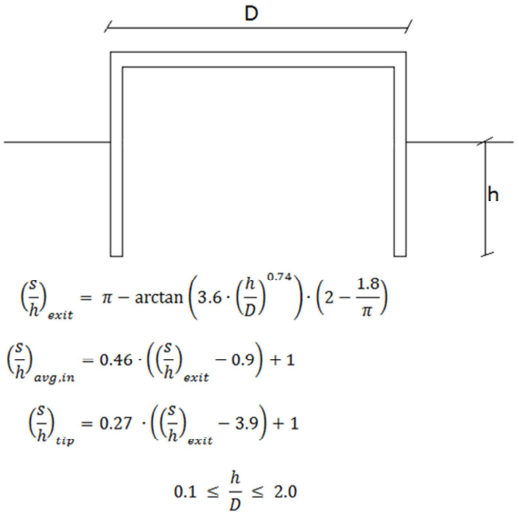

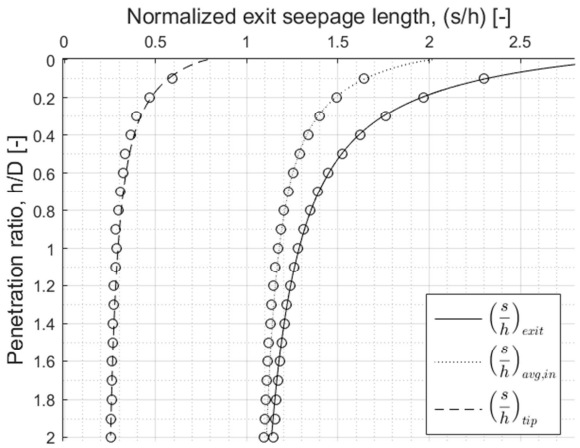

Figure 4.6. *Results of normalized seepage length for exit, average inside and tip gradients versus penetration ratio along with chosen solutions*

The normalized seepage length based on average hydraulic gradient outside the caisson is fitted to a linear function, *equation (4.4),* and the function is plotted in *Figure 4.7.*

$$\left(\frac{s}{h}\right)_{avg,out} = 4.8 \cdot \frac{h}{D} + 2.05 \tag{4.4}$$

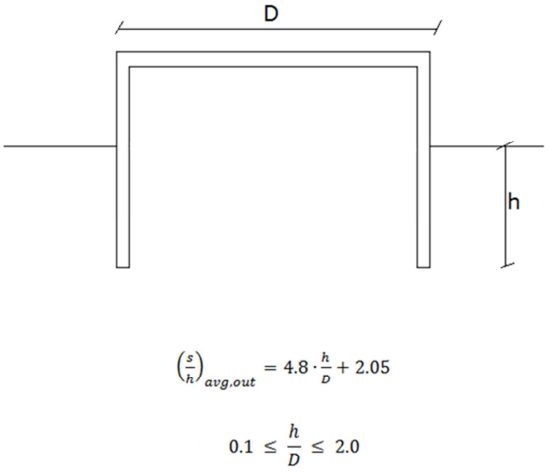

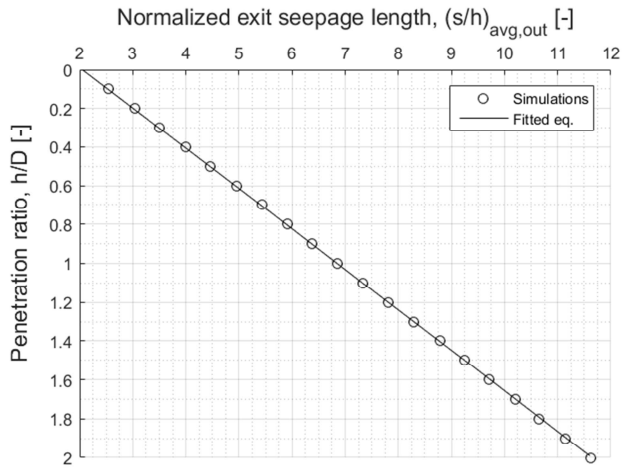

Figure 4.7. *Results of normalized seepage length for average outside gradient versus penetration ratio along with chosen solution*

4.2. Case of permeable soil overlaid by impermeable layer – closed top condition (b)

The soil profile used includes homogenies permeable soil, sand, under impermeable layer. The boundary conditions and model and soil properties are described in chapter 2. The theory used for deriving the results is described in chapter 3.

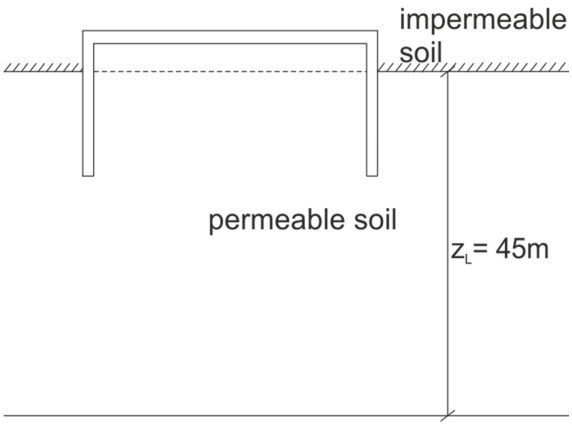

Figure 4.8. Case of homogenous permeable soil under impermeable soil layer

The graphs below show the excess pore pressure changes induced by suction for penetration ratio equal to 0.1, 0.5 and 1.0, *Figure 4.9.* It can be again concluded, that the hydraulic gradient at the inside skirt and at the tip is smaller for smaller penetration ratio. The impermeable layer situated above sand changes the seepage flow compared to case with only homogenies soil. The hydraulic gradients become less for small penetration ratio then it is for case (a). As a result less reduction in soil resistance is expected for the same applied suction. The further bucket penetrates, the less influence of impermeable layer is present, and flow is getting more similar to the case (a).

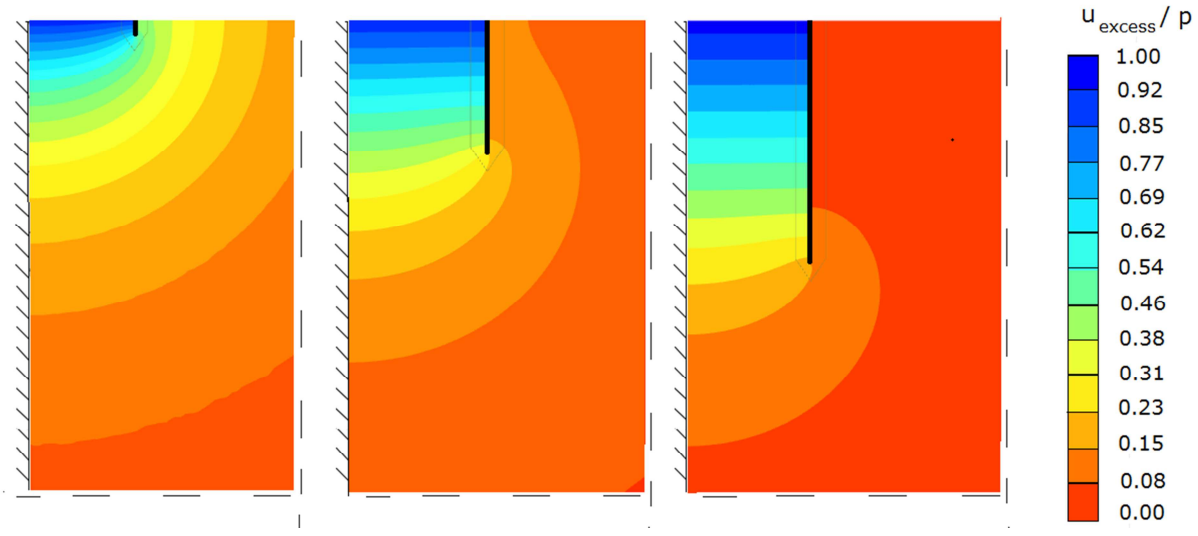

Figure 4.9. Results of ratio between excess pore pressure and applied suction under the bucket lid for $h/D = 0.1, 0.5$ and 1.0.

For the pore pressure factor, the same expression is used for fitting as in case (a). The constants for rational function are given below and the coefficient of determination is also high, $R^2 = 0.9997$.

a	0.21

b	0.24

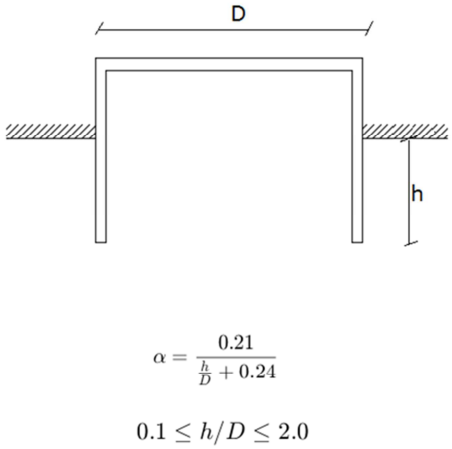

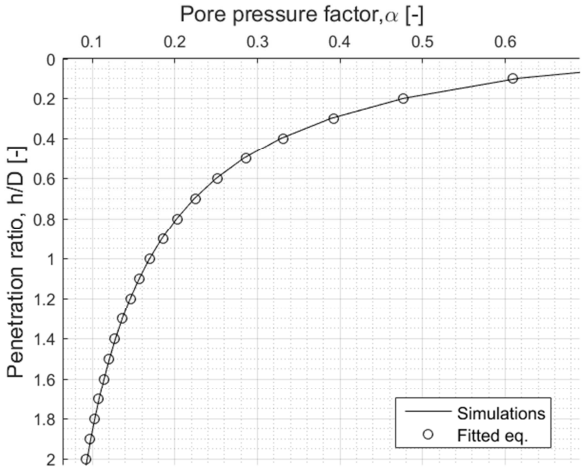

Figure 4.10. *Results of pore pressure factor versus penetration ratio along with chosen solution*

Results of normalized seepage length for case (b) differ significantly from the results of case 1 when the penetration ratio is small. With increasing the penetration depth, the influence of impermeable layer is getting less and less noticeable. Therefore, in order to find the best fit for numerical results, the reference expression for normalized seepage length is used and the difference is added throughout a power expression, see *equation (4.5)* , where the fit has a high coefficient of determination, $R^2 = 0.9987$.

$$\left(\frac{s}{h}\right)_{exit,closed\ top} = \frac{s}{h}_{ref} + 0.05 \cdot \frac{h}{D}^{-1.36} \tag{4.5}$$

The equation for normalized seepage length for exit gradient is used while fitting for average and tip gradients, as it was done in case (a), see *equation (4.6).* Constants found for both gradients and R^2 values are presented in *Table 4.2.*

$$\left(\frac{s}{h}\right) = a \cdot \left(\left(\frac{s}{h}\right)_{exit,closed\ top} - b\right) + 1 \tag{4.6}$$

Table 4.2. *Fitted constants for equation 4.2.2. and R^2values*

	for exit gradient	*for average gradient*	*for tip gradient*
a	1	0.64	0.33
b	1	1	3.4

R^2	0.9987	0.9905	0.9992

The results for closed top condition along with chosen solution are presented in *Figure 4.11.*

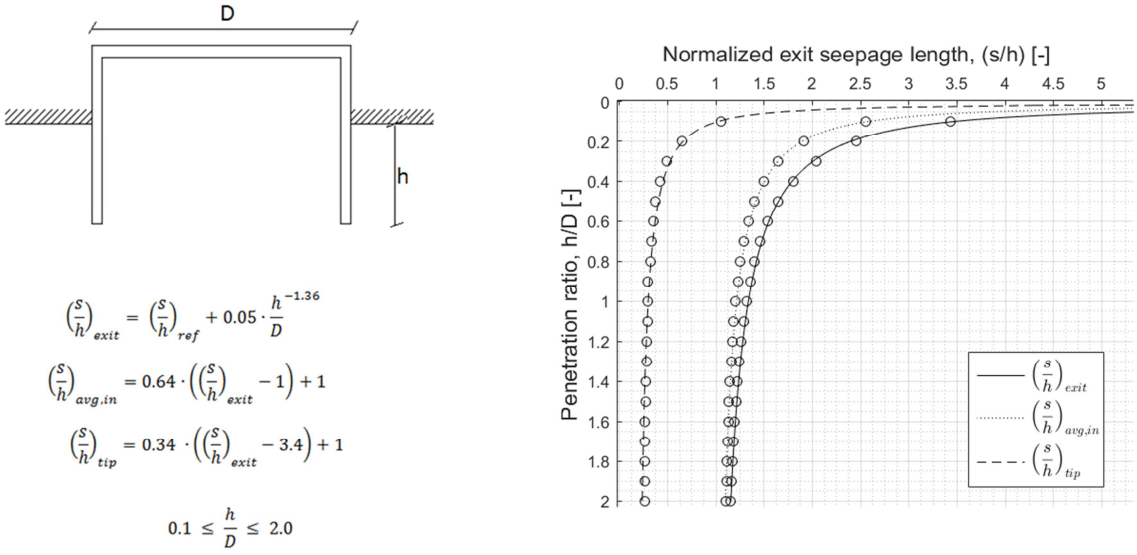

Figure 4.11. *Results of normalized seepage length for exit, average inside and tip gradients versus penetration ratio along with chosen solution*

The normalized seepage length based on average hydraulic gradient outside the caisson is close to linear for penetration ratio equal and more than 0.4, whereas the behavior is different for smaller penetration ratio. *Equation (4.7)* is found as a solution, with $R^2 = 0.9995$.

$$\left(\frac{s}{h}\right)_{avg,out} = \left(4.4 \cdot \frac{h}{D} + 4.35\right) + 5.3 \exp\left(-7.2 \cdot \frac{h}{D}\right) \quad (4.7)$$

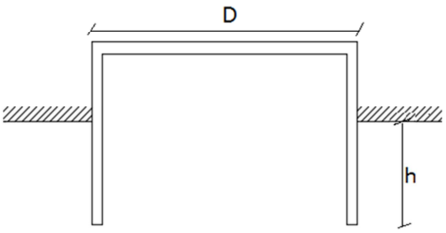

$$\left(\frac{s}{h}\right)_{avg,out} = \left(4.4 \cdot \frac{h}{D} + 4.35\right) + 5.3 \exp\left(-7.2 \cdot \frac{h}{D}\right)$$

$$0.1 \leq \frac{h}{D} \leq 2.0$$

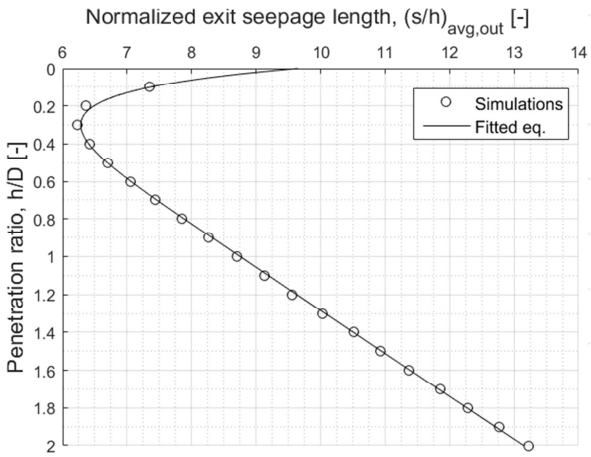

Figure 4.12. *Results of normalized seepage length for average outside gradient versus penetration ratio along with chosen solution*

4.3. Case of permeable soil over impermeable layer – closed bottom condition (c)

The soil profile used includes homogenies permeable soil, sand situated above impermeable layer. The boundary conditions and model and soil properties are described in chapter 2. The theory used for deriving the results is described in chapter 3.

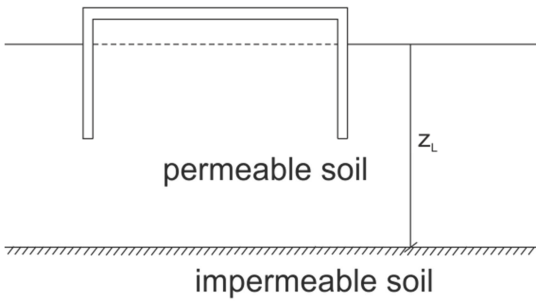

Figure 4.13. Case of homogenous permeable soil over impermeable soil layer

The graphs below show the excess pore pressure changes induced by suction for penetration ratio equal to 0.5 with different distances to impermeable layer below, *Figure 4.14.* It can be seen that the impermeable layer, situated closer to the tip of the bucket skirt, influences the hydraulic gradient on the inside wall. A lower gradient is induced when the distance to impermeable layer is smaller. Therefore, an increase in seepage length is expected when approaching impermeable layer, meaning that there will be almost no reduction in soil resistance. The further the impermeable layer is situated, the more similar the seepage conditions are to case with homogenies soil.

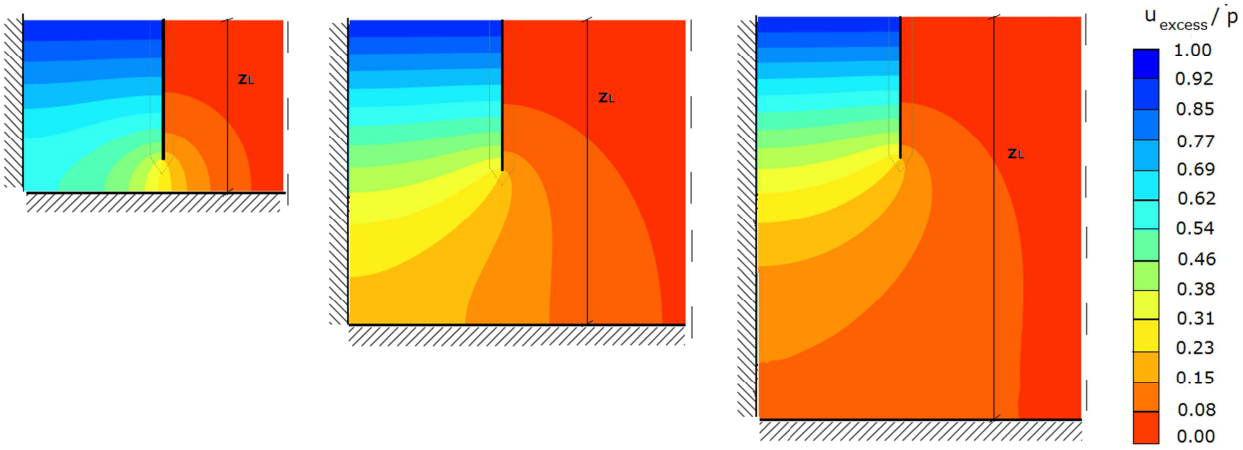

Figure 4.14. Results of ratio between excess pore pressure and applied suction under the bucket lid for $\frac{h}{D} = 0.5$ and $z_L/D = 0.6,\ 1.0$ and 1.4.

For pore pressure factor, the results obtained from numerical analysis are plotted together with function proposed by C. LeBlanc (Cotter, 2009), equation (3.5).

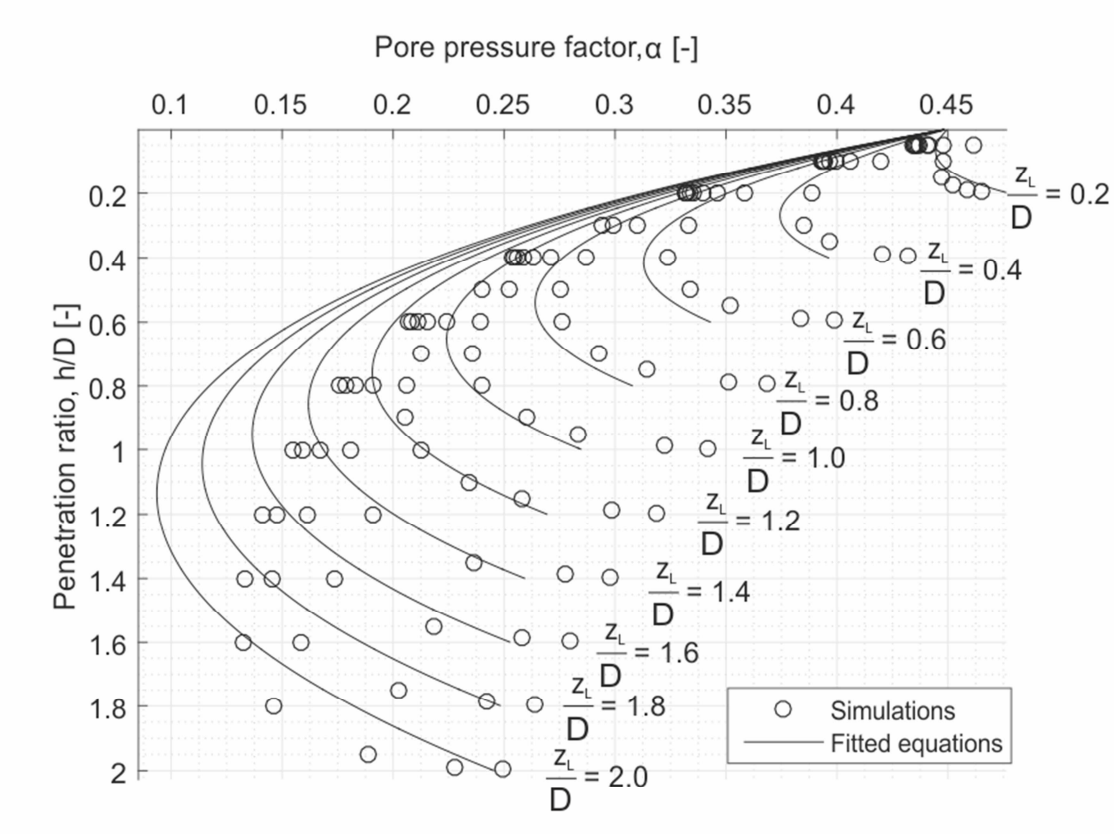

Figure 4.15. *Results of pore pressure factor versus penetration ratio along with equation (3.5)*

The coefficient of determination for each $\frac{z_L}{D}$ is shown in *Table 4.3.*

Table 4.3. *The coefficient of determination for cases with different distance to impermeable layer below permeable soil, equation (3.18)*

$\frac{z_L}{D}$	0.2	0.4	0.6	0.8	1.0	1.2	1.4	1.6	1.8	2.0
R^2	-1.41	0.34	0.67	0.85	0.92	0.94	0.95	0.95	0.93	0.91

The fit is not considered as a good fit. However, function somehow catches the main trend. Therefore, constants and exponent are individually fitted to all numerical data.

$$\alpha = \alpha_0 + a \cdot \frac{h}{D} \cdot \left(\left(\frac{h}{z_L} \right)^b + \frac{D}{z_L} - c \right) \tag{4.8}$$

The constants and exponent are then fitted to function in accordance to $\frac{z_L}{D}$ value. Results are presented in *Figure 4.16.* and the values of coefficients of determinations are given in *Table 4.4.*

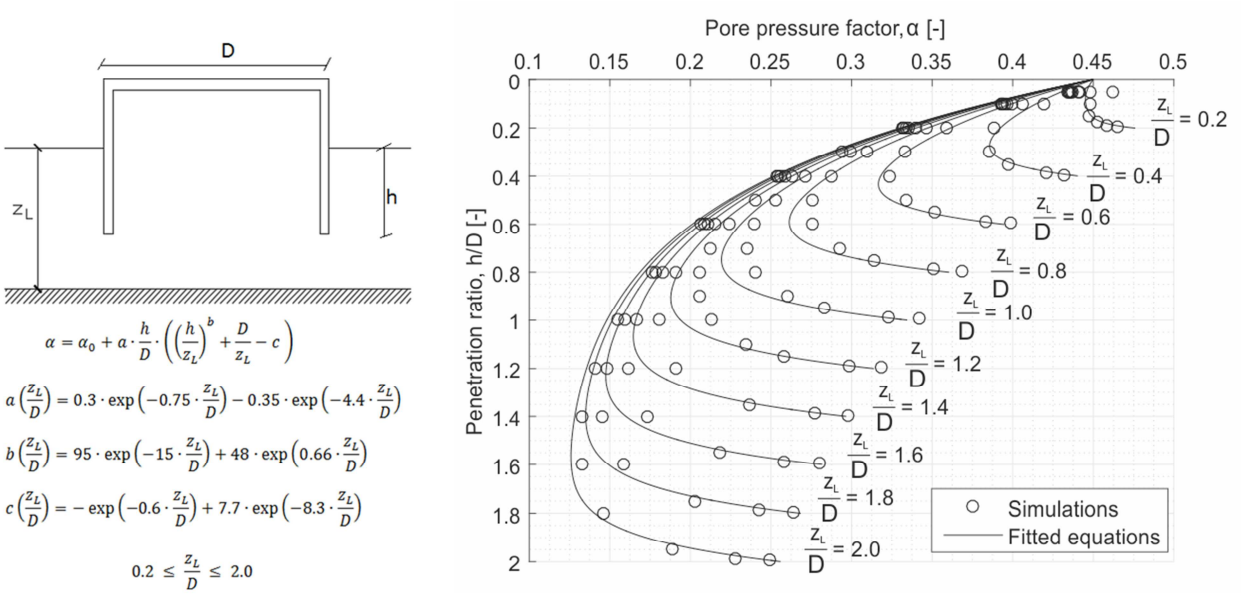

Figure 4.16. *Results of pore pressure factor versus penetration ratio along with chosen solution*

Table 4.4. *The coefficient of determination for cases with different distance to impermeable layer below permeable soil – with chosen solution*

$\frac{z_L}{D}$	0.2	0.4	0.6	0.8	1.0	1.2	1.4	1.6	1.8	2.0
R^2	0.91	0.98	0.98	0.97	0.96	0.95	0.95	0.95	0.95	0.95

The seepage length for closed bottom condition is found basing on the reference function from homogenies soil condition and the formulation found by (Ibsen and Thilsted, 2010). The expression is plotted along with PLAXIS results in *Figure 4.17*. and the coefficients of determination for each $\frac{z_L}{D}$ are in *Table 4.5.*

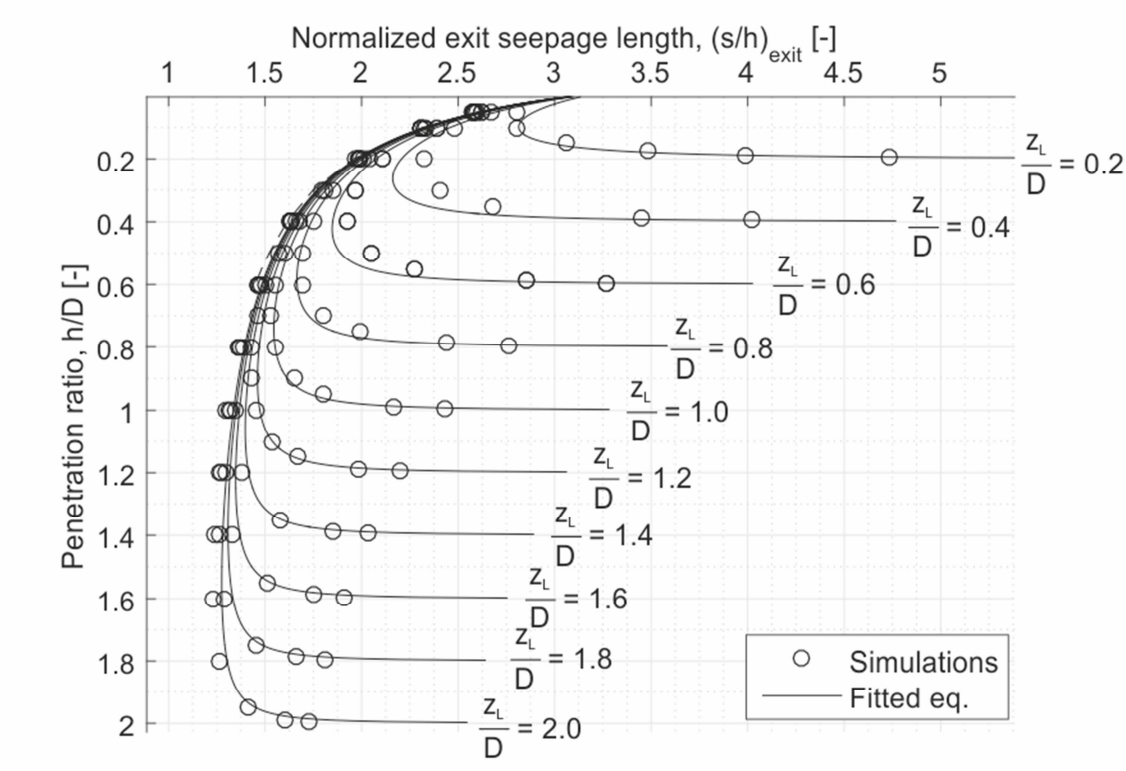

Figure 4.17. *Results of normalized seepage length for exit gradient versus penetration ratio along with solution from (Ibsen & Thilsted, 2010)*

Table 4.5. *The coefficient of determination for cases with different distance to impermeable layer below based on equation (3.24)*

$\frac{z_L}{D}$	0.2	0.4	0.6	0.8	1.0	1.2	1.4	1.6	1.8	2.0
R^2	0.94	0.83	0.91	0.96	0.95	0.93	0.91	0.91	0.91	0.81

The function captures the behavior trend. The constants from equation are adjusted to get the best fit, see *equation 4.9.* The results showed that the power parameter can be still fit as 0.5 and for the coefficient there is a new function in accordance to $\frac{z_L}{D}$.

$$\left(\frac{s}{h}\right)_{exit,closed\ bottom} = \left(\frac{s}{h}\right)_{ref} + a \cdot \left(\frac{D}{z_L}\right) \cdot \left(\frac{h}{z_L - h}\right)^{0.5} \tag{4.9}$$

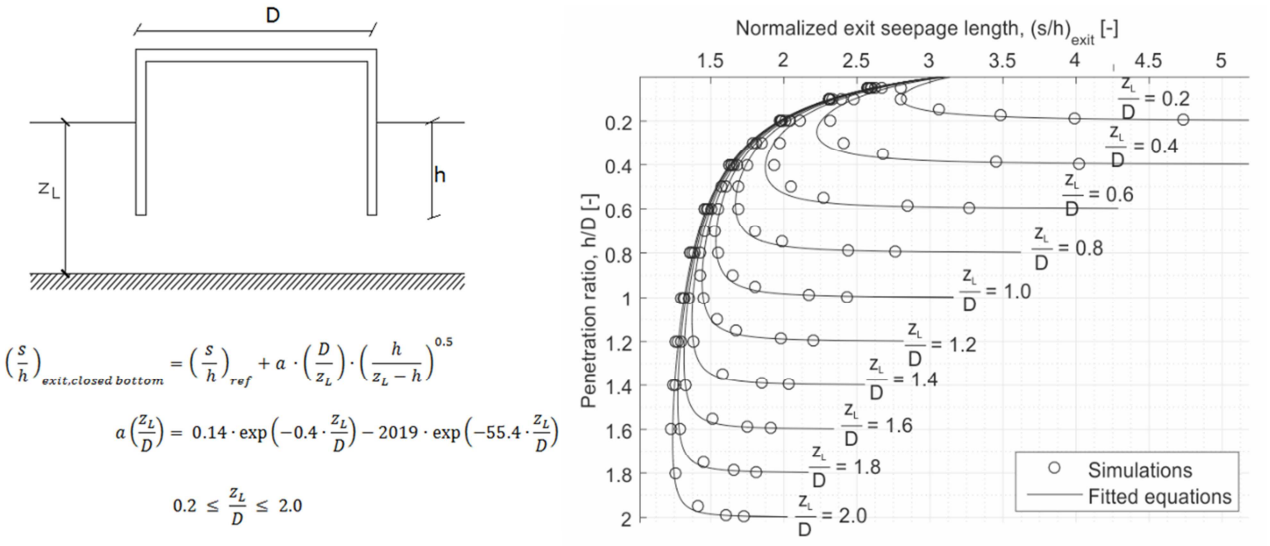

Figure 4.18. *Results of normalized seepage length for exit gradient versus penetration ratio along with chosen solution*

Table 4.6. *The coefficient of determination for cases with different distance to impermeable layer below for chosen solution*

$\frac{z_L}{D}$	0.2	0.4	0.6	0.8	1.0	1.2	1.4	1.6	1.8	2.0
R^2	0.95	0.93	0.94	0.95	0.97	0.98	0.98	0.99	0.99	0.99

As a normalized seepage is used to calculate the critical pressure, it can be deducted that the critical pressure is going to decrease with penetration ratio till the bucket will be penetrated into the permeable layer of 50% its depth for $\frac{z_L}{D} = 0.2$ up til 80% of its depth for $\frac{z_L}{D} = 2.0$. When approaching the impermeable layer there is an increase in critical pressure. The increase in critical pressure results in increase of β-factor, which means that there is less reduction in soil penetration resistance.

The normalized seepage length for the average inside hydraulic gradient first decreases with increasing penetration ratio, but when approaching closer to impermeable layer it starts to increase. This increase is less for small $\frac{z_L}{D}$ values and become more significant for increasing $\frac{z_L}{D}$ values. As a starting point for fitting equation (4.9) for exit gradient is considered. However, the data from simulation for average seepage length show that there is less increase of $\left(\frac{s}{h}\right)$ when approaching impermeable layer than it is for exit seepage length. Therefore the factor for curvature in equation (4.9) is adjusted.

$$\left(\frac{s}{h}\right)_{new} = \left(\frac{s}{h}\right)_{ref} + a \cdot \left(\frac{D}{z_L}\right) \cdot \left(\frac{h}{z_L - h}\right)^b \tag{4.10}$$

where

$$b\left(\frac{z_L}{D}\right) = 0.38 \cdot \exp\left(0.1 \cdot \frac{z_L}{D}\right) - 0.49 \cdot \exp(-3.6 \cdot \frac{z_L}{D}) \tag{4.11}$$

The expression for normalized seepage length for average inside gradient is finally:

$$\left(\frac{s}{h}\right)_{avg,in} = 0.46 \cdot \left(\left(\frac{s}{h}\right)_{new} - 0.9\right) + 1 \tag{4.12}$$

Table 4.7. *The coefficient of determination for normalized average seepage length based on equation (4.12)*

$\frac{z_L}{D}$	0.2	0.4	0.6	0.8	1.0	1.2	1.4	1.6	1.8	2.0
R^2	-4.99	0.54	0.79	0.91	0.94	0.97	0.98	0.99	0.99	0.99

The normalized seepage length for tip gradient behaves differently. There is more significant decrease in value for small penetration ratio and a significant decrease in value when approaching impermeable layer. The normalized tip seepage length is approaching value 0. As there is no increase at the end, therefore $\left(\frac{s}{h}\right)_{ref}$ for homogenies permeable layer, *equation (4.2)* is used in fitting process,

$$\left(\frac{s}{h}\right)_{tip} = a \cdot \left(\left(\frac{s}{h}\right)_{ref} - 3.9\right) + 1 \tag{4.13}$$

where

$$a\left(\frac{z_L}{D}\right) = 0.3 * \left(\frac{z_L}{D}\right)^{-0.1}. \quad (4.14)$$

Nevertheless, this function does not reflect the sudden decrease while approaching the impermeable layer. In fact there should be almost no penetration soil resistance when skirt penetrates close to the impermeable layer, resulting in less driving force requirements. The resistance against penetration in this case should be still investigated and confirmed by full-scale tests. However, using this solution leads to a safe design. From the same reason the values for coefficient of determination are smaller from desires.

Table 4.8. *The coefficient of determination for normalized tip seepage length based on equation 4.13.*

$\frac{z_L}{D}$	0.2	0.4	0.6	0.8	1.0	1.2	1.4	1.6	1.8	2.0
R^2	0.71	0.81	0.84	0.83	0.83	0.81	0.80	0.78	0.77	0.75

An example of normalized seepage length for exit, average and tip gradient for closed bottom case the situation with $\frac{z_L}{D}$ equal to 1.0 is chosen. Figures presenting average inside seepage, tip seepage and exit seepage for each $\frac{z_L}{D}$ value can be seen in Appendix A, page 46.

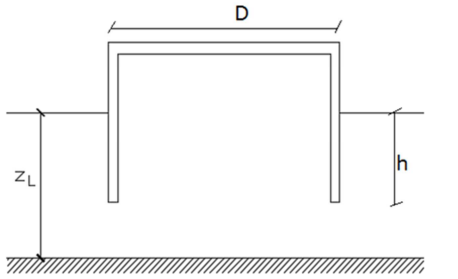

$$\left(\frac{s}{h}\right)_{avg,in} = 0.46 \cdot \left(\left(\frac{s}{h}\right)_{new} - 0.9\right) + 1$$

$$\left(\frac{s}{h}\right)_{new} = \left(\frac{s}{h}\right)_{ref} + a \cdot \left(\frac{D}{z_L}\right) \cdot \left(\frac{h}{z_L - h}\right)^b$$

$$a\left(\frac{z_L}{D}\right) = 0.14 \cdot \exp\left(-0.4 \cdot \frac{z_L}{D}\right) - 2019 \cdot \exp\left(-55.4 \cdot \frac{z_L}{D}\right)$$

$$b\left(\frac{z_L}{D}\right) = 0.38 \cdot \exp\left(0.1 \cdot \frac{z_L}{D}\right) - 0.49 \cdot \exp\left(-3.6 \cdot \frac{z_L}{D}\right)$$

$$0.2 \leq \frac{z_L}{D} \leq 2.0$$

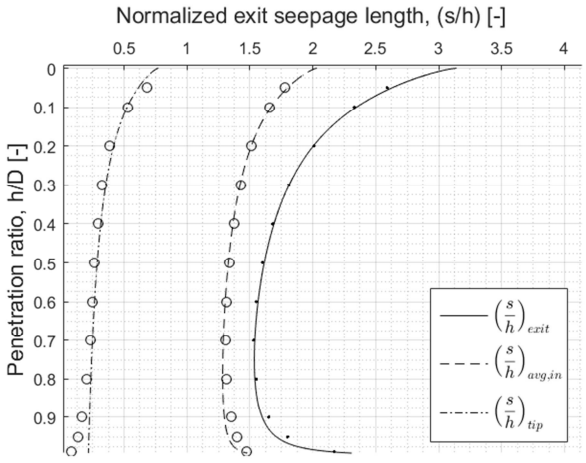

Figure 4.19. *Normalized seepage length for exit, average and tip gradient for closed bottom case for* $\frac{z_L}{D} = 1.0$*, with expression for normalized average seepage length*

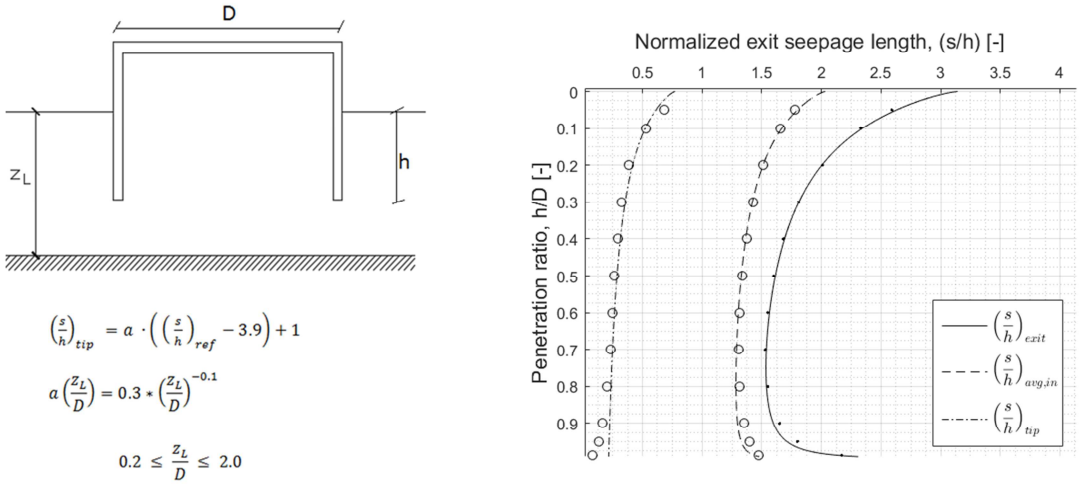

Figure 4.20. *Normalized seepage length for exit, average and tip gradient for closed bottom case for* $\frac{z_L}{D} = 1.0$*, with expression for normalize tip seepage length*

For the normalized seepage length for average outside gradient there is an increase or increasing penetration ratio, but when approaching impermeable layer, there is a significant decrease. The decrease is less visible for small $\frac{z_L}{D}$ values, and more major for large $\frac{z_L}{D}$ values. As a starting point for fitting function for outside normalized seepage from homogeneous case is used and adjusted.

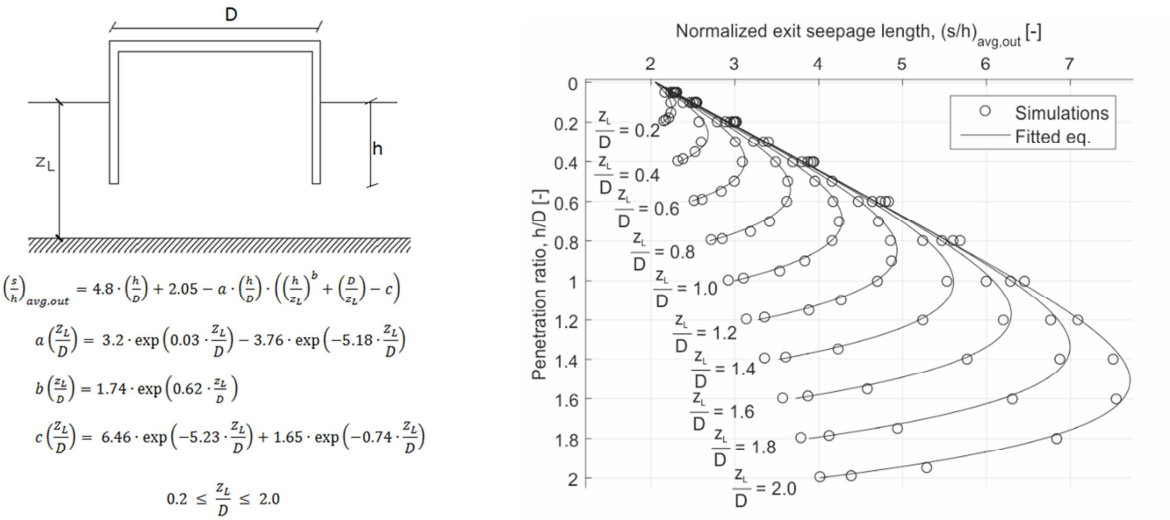

Figure 4.21. *Results of normalized seepage length for average outside gradient versus penetration ratio along with chosen solution*

5. Conclusions

The report presents the solutions for pore pressure factor and for normalized seepage length for the progressing process of installation of bucket foundation. The closed form solutions given in the rapport can be used when the soil conditions and bucket geometry is known. Three different soil profiles where considered: homogenies permeable soil, permeable soil under impermeable soil layer and permeable soil above impermeable soil layer.

Moreover, the method for installation procedure of bucket foundation is presented, from which the required suction for the installation can be predicted, including the changes in soil penetration resistance due to the seepage flow. Method is named AAU CPT-based method.

Concluding on results, the seepage flow inside the permeable layer behaves differently, if there is impermeable soil layer in close surroundings. Presence of impermeable layer above sandy soil, as well as presence of impermeable layer below, increases the normalized seepage length value and the pore pressure factor. Exception from this are the results of normalized seepage length for tip gradient for the case when penetrating skirt approaches the impermeable layer, case (c). In this case the values are decreasing towards 0, indicating almost full reduction in tip resistance in short time and for relatively small values of applied suction.

The results proves that the critical gradient due to applied suction under the bucket lead occurs first at the tip, then along the inside wall and finally at the exit, inside the bucket. According to numerical results, it is the soil resistance at the tip, which is reduced the most. It might seem logical then, that the failure of soil could happen in the same time. However, it is predicted that the soil material in surroundings densifies the area around the tip and therefore, it is the exit seepage results that should be controlling the allowable suction in order to avoid complete loosening of sand, resulting in piping channels.

The proposed solution getting us closer to the full design of installation of bucket foundation in permeable soil, where also impermeable soil layer are present in soil profiles. The study requires still closed form solutions for soil with different coefficient of permeability, somehow lower that the one for sand, and higher than values for impermeable soil. The research should also include different rates of installation. Such a numerical analysis is expected to be performed as a next step of this study.

Finally, the solutions that are proposed, based on numerical investigation, require a confirmation and adjustments with results of full-scale tests. The final results of the study should give a full design method for bucket foundation installation in different soil conditions and with different penetration rates. The design will include the critical suction estimation and the possibility to predict the reduction in soil penetration resistance as an effect of pore water flow in the soil.

6. References

Brinkgreve, R. E. (2012). Plaxis 2D, Reference Manual. Netherland: PLAXIS bv.

Cotter, O. (2009). *The installation of suction caisson foundations for offshore renewable energy structures.* Oxford: University of Oxford.

DNV. (1992). *DNV - Foundation, classification notes No 30.4.* Høvik, Norway: Det Norske Veritas.

Feld, T. (2001). *Suction Buckets: a new innovation foundation concept, applied to offshore wind turbines.* Aalborg: Aalborg Universitetsforlag.

Houlsby, G. T., & Byrne, B. W. (2005). Design procedures for installation of suction caissons in sand. *Proceedings of the ICE - Geotechnical Engineering*, *158*(GE3), 135–144. http://doi.org/10.1680/geng.2005.158.3.135

Houlsby, G. T., Ibsen, L. B., & Byrne, B. W. (2005). Suction caissons for wind turbines. *Frontiers in Offshore Geotechnics: Proceedings of the International Symposium. on Frontiers in Offshore Geotechnics (IS-FOG 2005), 19-21 Sept 2005, Perth, WA, Australia*, 75–93. Retrieved from http://www.eng.ox.ac.uk/civil/people/bwb-1/papers/isfog_1.pdf

Ibsen, L. B., & Thilsted, C. L. (2010). Numerical Study of Piping Limits for Suction Installation of Offshore Skirted Foundations an Anchors in Layered Sand. *Frontiers in Offshore Geotechnics*, *II*, 421–426.

Senders, M., & Randolph, M. F. (2009). CPT-Based Method for the Installation of Suction Caissons in Sand. *Journal of Geotechnical and Geoenvironmental Engineering*, *135*(January), 14–25. doi:10.1061/(ASCE)1090-0241(2009)135:1(14)

Tran, M. (2006). *Installation of suction caissons in dense sand and the influence of silt and cemented layers.* Sydney: University of Sydney, School of Civil Engineering.

II. Appendix

A. Results of average inside, tip and exit normalized seepage for closed bottom condition for each $\frac{z_L}{D}$ value

The closed bottom condition, sand over impermeable soil, for each $\frac{z_L}{D}$ value are presented below.

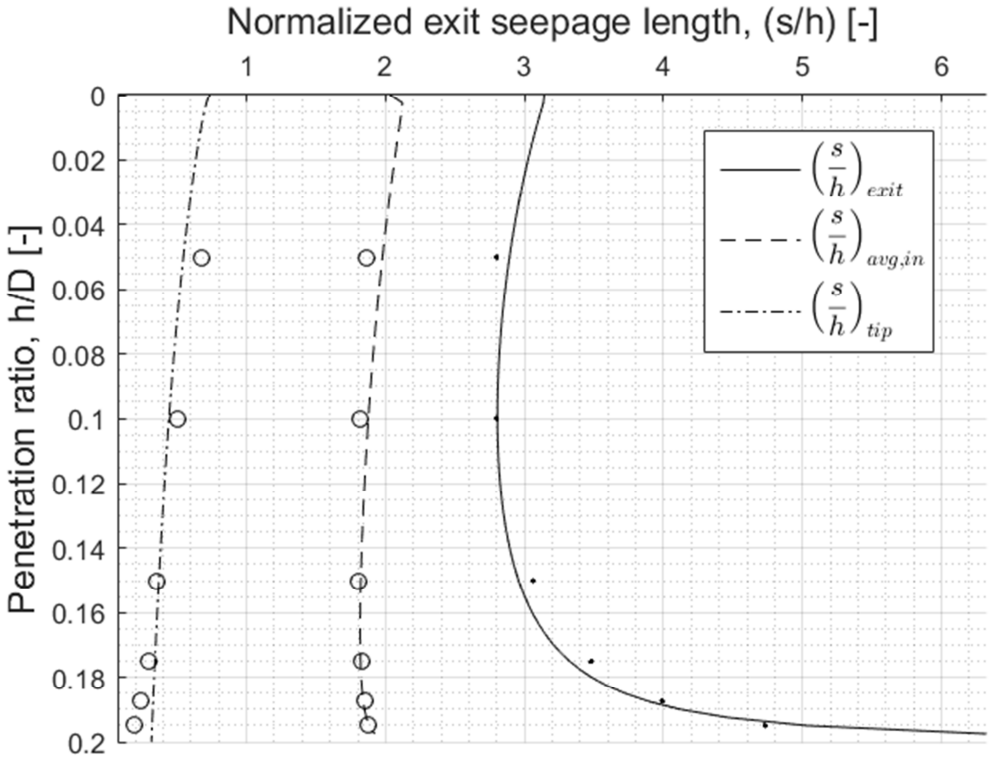

Figure A.1. Normalized seepage for exit, average outside and tip gradient for closed bottom case, $\frac{z_L}{D} = \mathbf{0.2}$

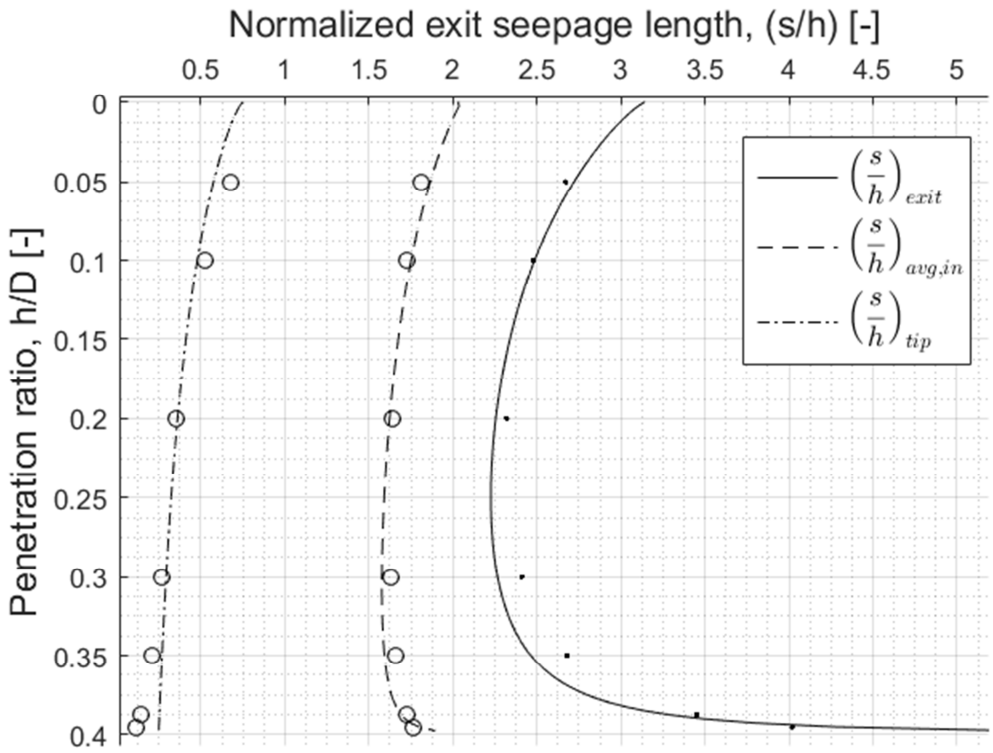

Figure A.2. Normalized seepage for exit, average outside and tip gradient for closed bottom case, $\frac{z_L}{D} = \mathbf{0.4}$

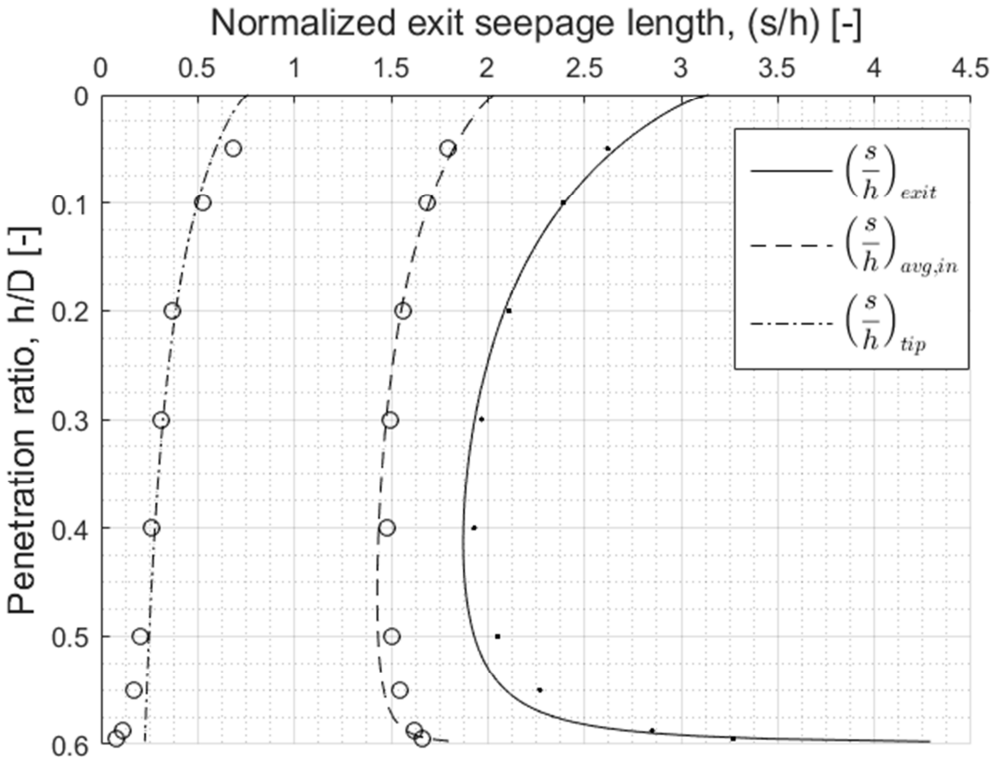

Figure A.3. Normalized seepage for exit, average outside and tip gradient for closed bottom case, $\frac{z_L}{D} = \mathbf{0.6}$

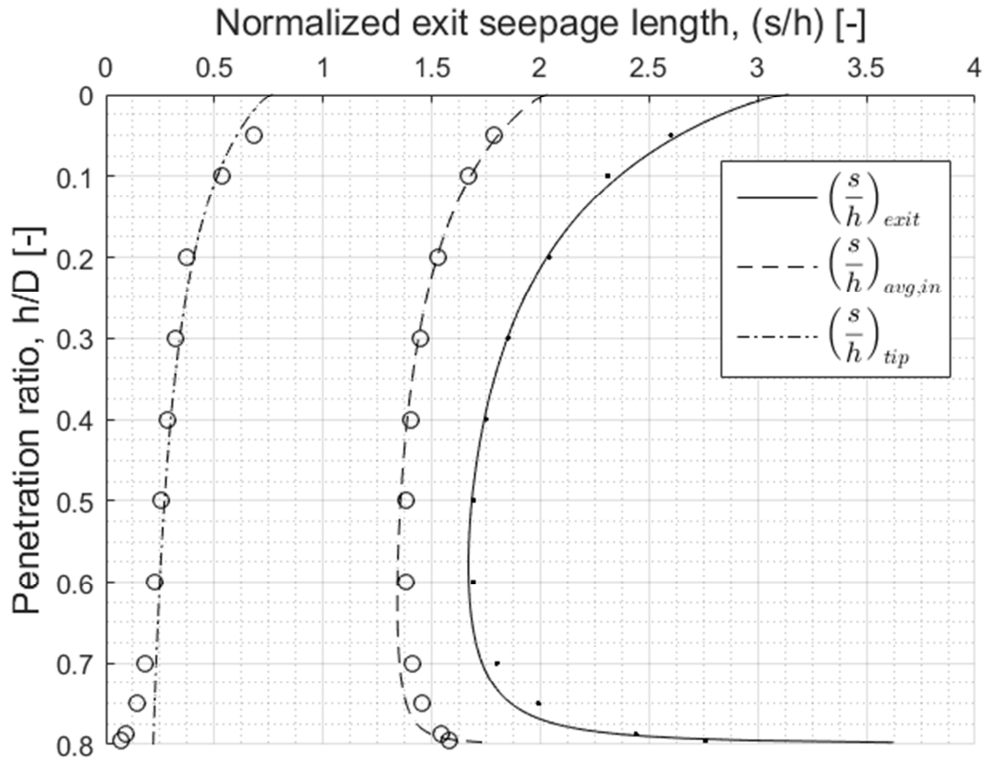

Figure A.4. Normalized seepage for exit, average outside and tip gradient for closed bottom case, $\frac{z_L}{D} = \mathbf{0.8}$

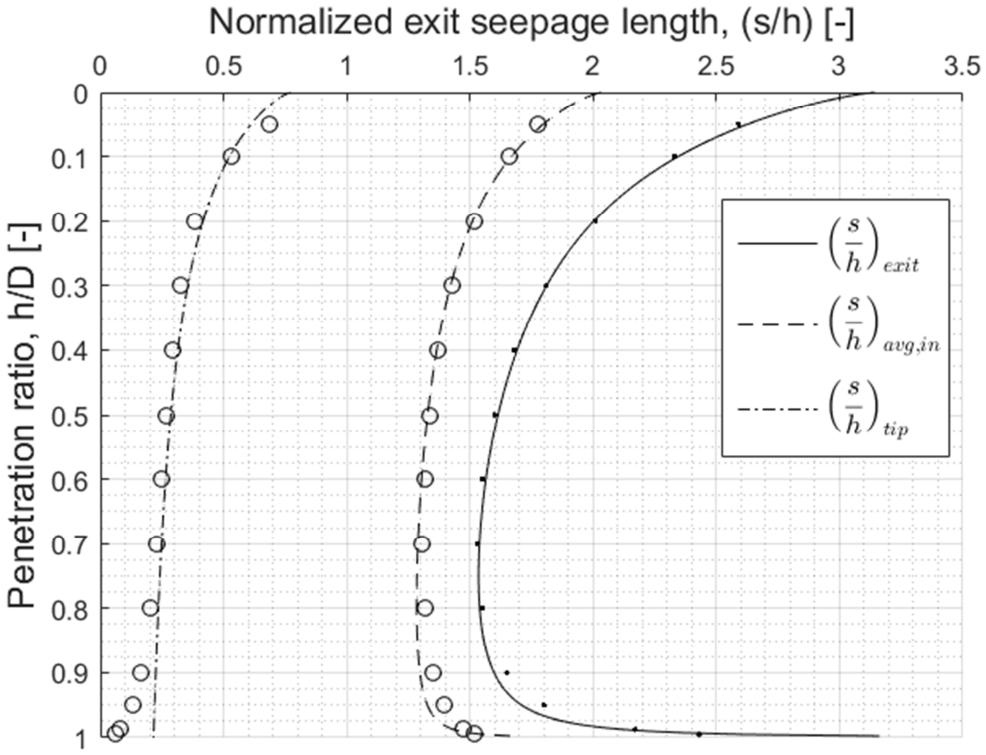

Figure A.5. Normalized seepage for exit, average outside and tip gradient for closed bottom case, $\frac{z_L}{D} = \mathbf{1.0}$

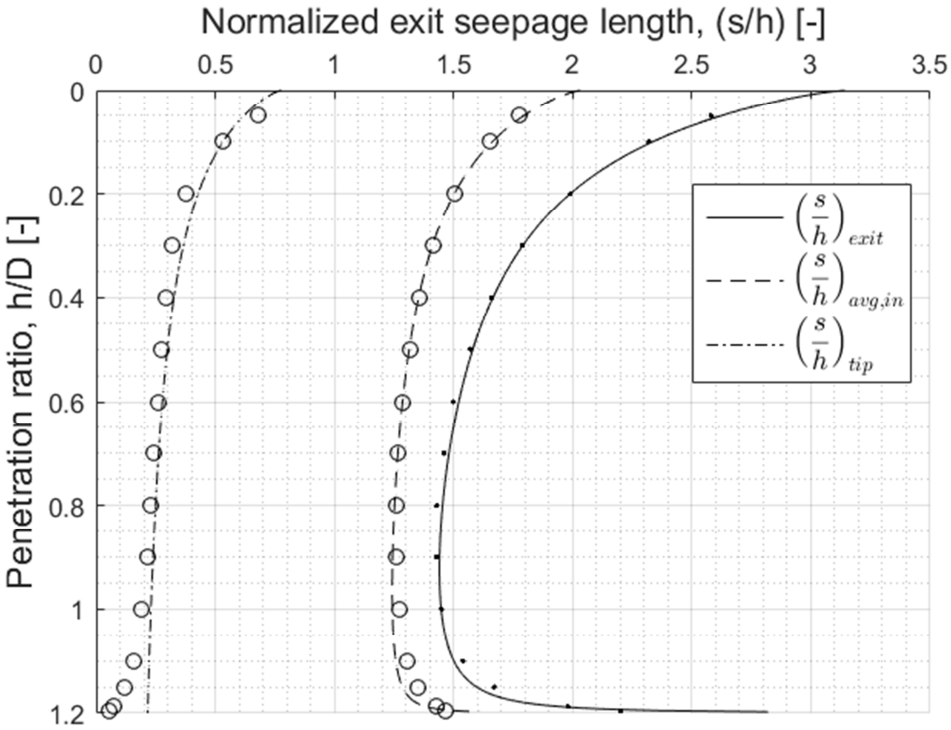

Figure A.6. Normalized seepage for exit, average outside and tip gradient for closed bottom case, $\frac{z_L}{D} = \mathbf{1.2}$

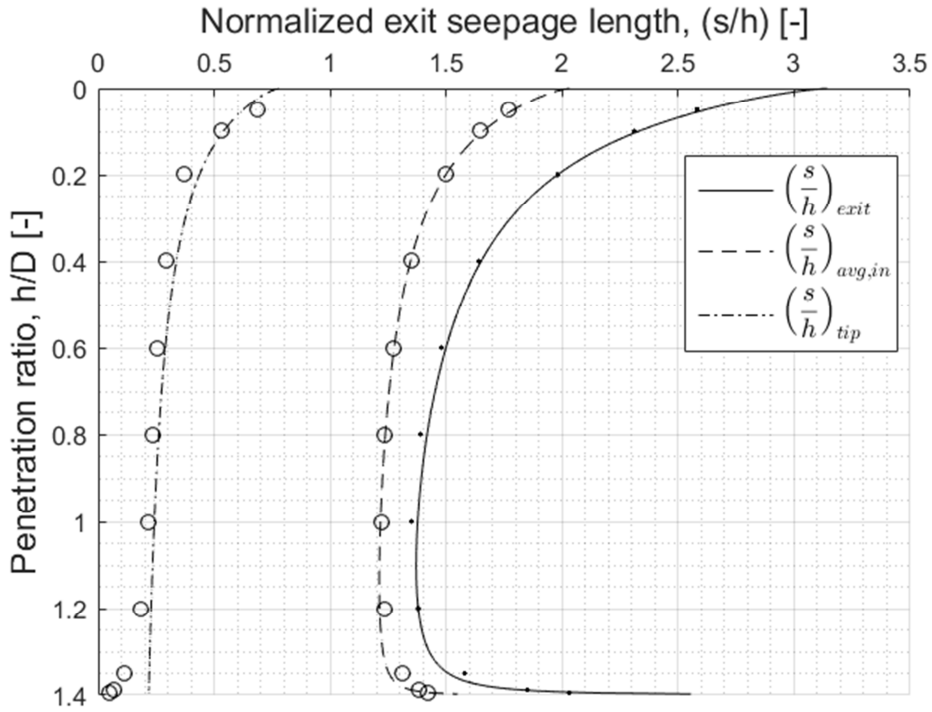

Figure A.7. Normalized seepage for exit, average outside and tip gradient for closed bottom case, $\frac{z_L}{D} = \mathbf{1.4}$

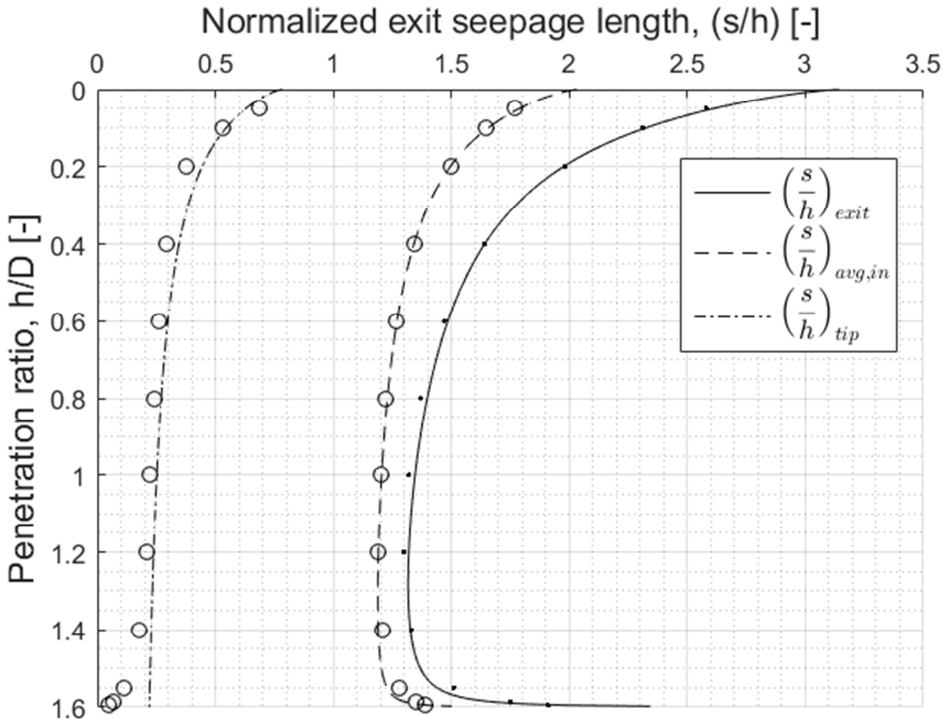

Figure A.8. Normalized seepage for exit, average outside and tip gradient for closed bottom case, $\frac{z_L}{D} = \mathbf{1.6}$

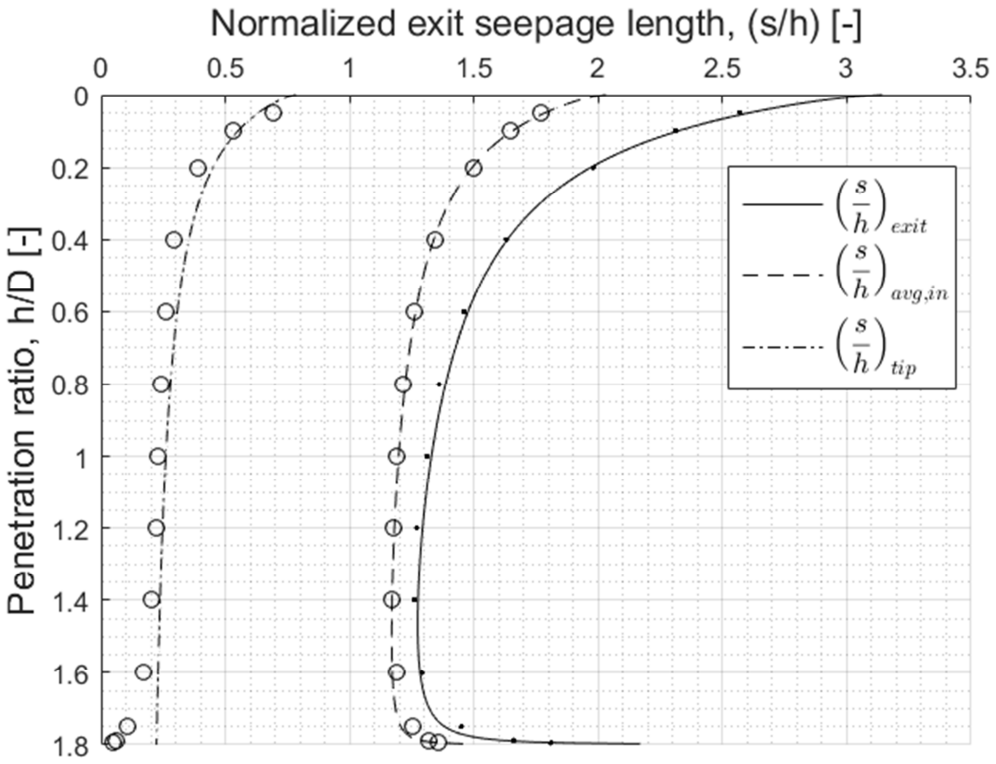

Figure A.9. Normalized seepage for exit, average outside and tip gradient for closed bottom case, $\frac{z_L}{D} = \mathbf{1.8}$

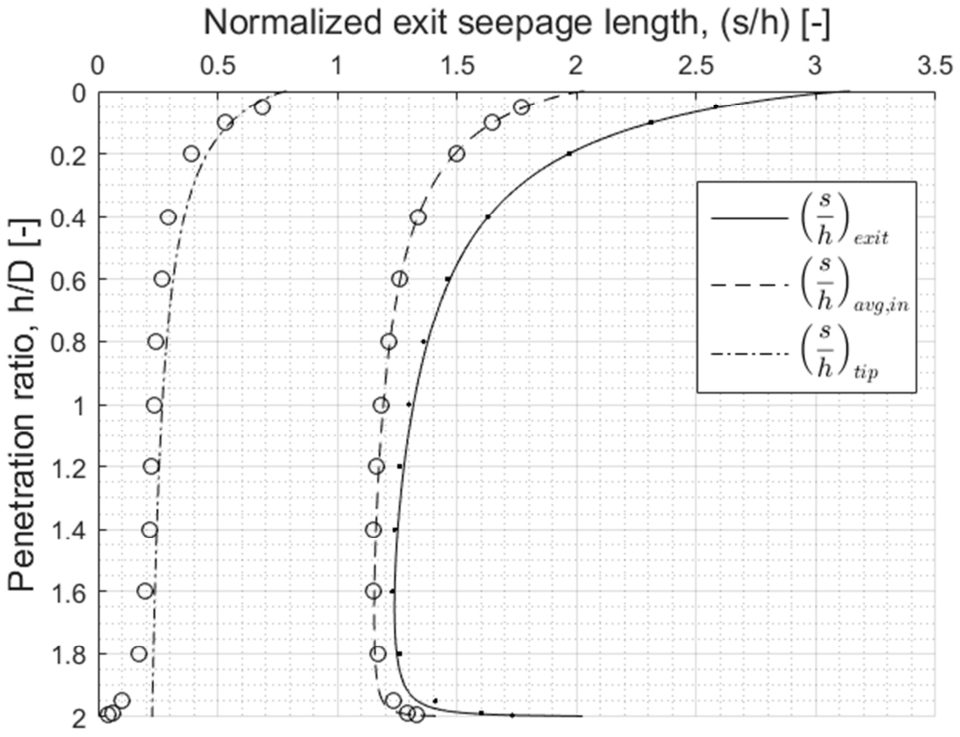

Figure A.10. Normalized seepage for exit, average outside and tip gradient for closed bottom case, $\frac{z_L}{D} = \mathbf{2.0}$

Recent publications in the DCE Technical Memorandum Series

ISSN 1901-7278

DCE Technical Memorandum No. 52